Plasma Metabolomic Profiles and Clinical Features in Recovered COVID-19 Patients Without Previous Underlying Diseases 3 Months After Discharge

Sufei Wang
NHC Key Laboratory of Pulmonary Diseases, Union Hospital, Tongji Medical College, Huazhong University of Science and Technology
Juanjuan Xu
NHC Key Laboratory of Pulmonary Diseases, Union Hospital, Tongji Medical College, Huazhong University of Science and Technology
Ping Luo
Union Hospital, Tongji Medical College, Huazhong University of Science and Technology,
Lian Yang
Union Hospital, Tongji Medical College, Huazhong University of Science and Technology
Siwei Song
NHC Key Laboratory of Pulmonary Diseases, Union Hospital, Tongji Medical College, Huazhong University of Science and Technology
Xueyun Tan
NHC Key Laboratory of Pulmonary Diseases, Union Hospital, Tongji Medical College, Huazhong University of Science and Technology
Qing Chen
Union Hospital, Tongji Medical College, Huazhong University of Science and Technology
Hui Xia
NHC Key Laboratory of Pulmonary Diseases, Union Hospital, Tongji Medical College, Huazhong University of Science and Technology
Shujing Zhang
NHC Key Laboratory of Pulmonary Diseases, Union Hospital, Tongji Medical College, Huazhong University of Science and Technology
Pei Ma
NHC Key Laboratory of Pulmonary Diseases, Union Hospital, Tongji Medical College, Huazhong University of Science and Technology
Yanling Ma
NHC Key Laboratory of Pulmonary Diseases, Union Hospital, Tongji Medical College, Huazhong University of Science and Technology
Fan Yang
Union Hospital, Tongji Medical College, Huazhong University of Science and Technology
Yu Liu
Union Hospital, Tongji Medical College, Huazhong University of Science and Technology
Yumei Li
NHC Key Laboratory of Pulmonary Diseases, Union Hospital, Tongji Medical College, Huazhong University of Science and Technology
Guanzhou Ma
NHC Key Laboratory of Pulmonary Diseases, Union Hospital, Tongji Medical College, Huazhong University of Science and Technology
Zhihui Wang
Union Hospital, Tongji Medical College, Huazhong University of Science and Technology
Yanran Duan
Tongji Medical College, Huazhong University of Science and Technology
Yang Jin (whuhjy@126.com)
NHC Key Laboratory of Pulmonary Diseases, Union Hospital, Tongji Medical College, Huazhong University of Science and Technology

Research Article

Keywords: COVID-19, Metabolomic profiles, Recovered patients, Metabolism

Posted Date: November 20th, 2020

DOI: https://doi.org/10.21203/rs.3.rs-110981/v1

Abstract

Knowing the residual and future effect of SARS-CoV-2 on recovered COVID-19 patients is critical for optimized long-term patient management. Recent studies focus on the symptoms and clinical indices of recovered patients, but the pathophysiological change is still unclear. To address this question, we examined the metabolomic profiles of recovered asymptomatic (RA), moderate (RM) and severe and critical (RC) patients without previous underlying diseases discharged from the hospital for 3 months, along with laboratory and CT findings. We found that the serum metabolic profiles in recovered COVID-19 patients still conspicuously differed from that in healthy control (HC), especially in the RM, and RC patients. Additionally, these changes bore close relationship with the function of pulmonary, renal, hepatic, microbial and energetic metabolism and inflammation. These findings suggested that RM and RC patients sustained multi-organ and multi-system damage and these patients should be followed up on regular basis for possible organ and system damage.

Introduction

The coronavirus disease 2019 (COVID-19), caused by severe acute respiratory syndrome coronavirus 2 (SARS-CoV-2), has claimed 27 million people and more might fall victims to it because of its high transmission. Recent studies showed that some recovered patients still have symptoms or develop new ones, such as shortness of breath, general fatigue, pulmonary fibrosis, [1] cardiac injury, [2,3] olfactory impairment, [4] plus abnormal laboratory indicators[2] in the early recovery stage. Nonetheless, our understanding remains poor in the residual and future impact of the viral infection on the recovered patients.

Metabolic processes are intimately correlated to the pathogenesis of a condition and its resulting pathology and pathophysiology and the host response to the infection. Small molecular metabolites, as the downstream products of genes and proteins, are closely related to the phenotype, and can accurately reflect subtle changes and potential impact under the biological state. [5] Metabolic changes in plasma have been previously reported for different viral infections, such as infection with SARS, [6] H1N1, [7] respiratory syncytial virus, [8] Ebola virus[9] and dengue. [10] Recent studies revealed metabolic dysregulation in COVID-19 patients and metabolites may help stratify patients in term of disease severity during hospitalization. [11-13] Moreover, discharged COVID-19 patients were also found to have disordered plasma metabolism. [12] Therefore, understanding of metabolic changes in recovered COVID-19 patients may help us find clues to the physiological and pathophysiological processes during rehabilitation and better manage recovered COVID-19 patients.

In this study, we ruled out the effects of the acute phase of the SARS-CoV-2 and selected recovered patients 3 months after discharge. We also eliminated the metabolic interference of other underlying diseases and only observed the residual effects of SARS-CoV-2 on patients. Finally, we divided patients into four groups in terms of their severities. We determined the metabolome to examine the potential effects of SARS-CoV-2 on recovered patients. We quantitatively determined the plasma lipidome and metabolome in a prospective cohort (NCT04283396) of 135 subjects, including 39 HC and 96 recovered COVID-19 patients of various severities (i.e., 18 RA, 34 RM, 44 RC patients) who were discharged 3 months ago. Meanwhile, blood biochemical indexes and chest CT scanning were studied to assess their clinical recovery. Clinical data suggested that RA patients recovered well but in RM and RC patients some parameters were still abnormal as compared with HC. Our findings demonstrated that the plasma metabolic alterations progressed gradually in RA, RM and RC patients when compared with HC. Correlation analysis revealed that many differential metabolites were closely associated with the function of pulmonary, renal, hepatic, microbial and energetic metabolism and inflammation, indicating RM and RC patients may take more time to recover from SARS-CoV-2-caused damage.

Results

1. Demographic and clinical features of recovered COVID-19 patients

A total of 135 samples, from 39 HC, 18 RA, 34 RM and 44 RC patients without underlying diseases who had been discharged 3 months ago, were enrolled (Figure 1). As shown in Table 1, all recovered patients tested positive for IgG or/and IgM, suggesting humoral immunity played an important role in their recovery. [14] Results of blood routine, blood biochemistry and coagulation function tests are listed in Table 1. Compared with HC, AST level was only marginally elevated in RA patients. In RM or RC patients, factors indicative of poor prognosis, such as lymphopenia, eosinopenia, increased LDH level, AST and glucose level[15-17] returned to normal compared to HC. However, laboratory parameters related to immune system (WBC, neutrophils), liver function (ALT, ALP), renal function (creatinine, uric acid) and cardiac injury (CK-MB) remained aberrant in RM or RC patients compared to HC. We also identified some new changes. Different from the results at admission, WBC and neutrophil cells decreased and uric acid (UA) level increased in RC patients when compared to HC.

Besides, a total of 26 HC and 90 recovered COVID-19 patients (18 in RA group, 33 in RM group and 39 in RC group) underwent chest CT under this trial. Representative CT images of different groups are shown in Figure 2 A-D. Chest CT exhibited that patients in recovered groups had lesions in lungs (Table 2). Of the 33 RM patients, 19 (57.58%) had residual lung lesions and/or subpleural lesions. Of the 39 RC patients, 26 (66.67%) had residual lung lesions and/or subpleural lesions. There was no significant difference in chest CT findings between RA patients and HC (all $P > 0.05$). Ground glass opacity (GGO), the most common radiological abnormality revealed at admission, was still significantly more in RM (51.52%,

P <0.05) and RC (48.72%, P <0.05) patients compared with HC (15.38%). Other radiological features including fibrous stripe, thickening of the adjacent pleura and bronchovesicular bundle distortion, were also significantly more apparent in RC patients compared with HC. AI-derived CT features quantifying pneumonia lesions were studied to assess the rehabilitation of lung (Figure 2E, Table 2). PGV and PCV, two promising non-invasive prognostic indicators, could early predict the progression of COVID-19 to severe illness. [18] There was no significant difference in pneumonia lesions (PGV, PCV and PLV) between HC and RA patients (Table 2, P >0.05). However, PGV, PCV and PLV in the whole lung or left/right lobe in RC patients were significantly different from those in HC (P <0.05). In RM patients, except for PCV of left lobe (P = 0.11), other pneumonia lesions were significantly different from those in HC (P <0.05). All aforementioned findings indicated that the impact of COVID-19 on lung persisted in RM and RC patients. Moreover, the results also suggested that RA patients recovered well and RM or RC patients did not recover from the pathological impacts of COVID-19.

2 Recovered COVID-19 patients presented plasma metabolic profiles that were different from healthy control

A total of 332 metabolites, including amino acids, bile acids, organic acids, acylcarnitines (ACNs), steroids, amides and some lipid species, were determined in the 135 subjects by using untargeted LC-MS method. In the PLS-DA scores plot, the plasma samples from RM and RC patients clustered well and were away from the HC (Figure 3A), which indicated that the metabolic profiles of RM and RC patients were remarkably different from those of HC. Consistently, the levels of 65 and 87 metabolites in RM and RC patients were significantly different from those in HC (Figure 3B, Table S1). Additionally, the samples of RA and HC were mingled in the PLS-DA scores plot, and only 17 metabolites altered significantly in RA patients (Figure 3A, B), illustrating the differences was small in metabolic profiles between the two groups.

Among these differential metabolites, 25 metabolites showed comparable changes in RM and RC groups, such as the decreased taurine, succinate, hypoxanthine, inosine, Adenosine 3', 5'-cyclic monophosphate (cyclic AMP), hippurate, and increased aconitate, dihydroxymandelic acid, abscisate, inosine-5-monophosphate (IMP). However, most metabolite changes were unique in each group (Figure 3B, and Figure 4A). For example, homotyrosine, indoleacetate, indolelactate, indole-3-carboxylate, methylindole, glycocholic acid (GCA), palmitic acid, heptadecanoic acid, riboflavin, and some glycerophospholipids of phosphatidylcholine (PC), and phosphatidylethanolamines (PE) were significantly decreased only in the RC group. While amino acids of phenylalanine, methionine, leucine, betaine, homothreonine, hydroxybenzoic acid, niacinamide, citramailc acid, hydroxyisocaproate, butyrylcarnitine (ACN C4:0), glycoursodeoxycholic acid (GUDCA) were significantly decreased only in the RM group. Gentisate, urate, 3-amino-5-methylhexanoate (AMH), pantothenate, free carnitine, arginine, choline, chenodeoxycholic acid (CDCA), oleic acid, aspartate, ribitol, lactoylglutathione were elevated only in the RC group.

To further understand these metabolic changes, pathway analysis was performed to know the biological implications of these differential metabolites. These metabolic disorders mainly involved alanine, aspartate and glutamate metabolism, citrate cycle (TCA cycle), purine metabolism, arginine biosynthesis, glycerophospholipid metabolism, glyoxylate and dicarboxylate metabolism (Figure 4B-C) in the RM and RC patients. We found some metabolic abnormalities even at the time of SARS-CoV-2 infection. And previous studies revealed disordered metabolism of tricarboxylic acid (TCA), purines and lipids in COVID-19 patients. In our study, we found these pathways were still disturbed in the recovered COVID-19 patients when compared with the HC, especially in the RC patients. We also found some new metabolic abnormalities during their convalescent phase, and metabolite changes were more related to microbial metabolism in the RC patients, such as decreased indoleacetate, indole-3-carboxylate.

Of note, the metabolic alterations progressed incrementally in RA, RM and RC patients when compared with HC (Figure 3C-E), indicating that the infection of SARS-CoV-2 still affects their recovery of plasma metabolite profiles in the convalescent phase. Previous studies revealed that the plasma metabolome of moderate, and severe and critical patients did not return to normal at discharge. Furthermore, we found that, even 3 months after discharge, multiple differences in plasma metabolites remained between patients and HC, suggesting that the RM and RC patients may require more time to recuperate from the impact of SARS-CoV-2 infection.

3 Differential metabolites exhibited that the SARS-CoV-2 exerted a persistent impact on organ and system in recovered patients

To understand the mechanism of the metabolite changes in recovered COVID-19 patients, the relationships between these differential metabolites and clinical parameters were investigated by examining the correlation among HC, RM and RC COVID-19 patients. Only correlations with $p < 0.05$, correlation coefficients > 0.3 or <-0.3 are displayed in the network of interactions (Figure 5). As expected, the clinical indexes bore complex relationships with the differential metabolites. For instance, the levels of γ-GT, α-HBDH, uric acid (UA), and WBC were significantly correlated with the levels of 39, 31, 32, and 33 metabolites, respectively (Figure 5A). Additionally, most of altered metabolites, such as cyclic AMP, homotyrosine, ACN 8:0, PC 38:5, were closely associated with these clinical indexes (Figure 5A). It was worth noting that many of these relationships significantly differed between HC and recovered COVID-19 patients.

Chest CT

As displayed in Figure 5B, many unique or characteristic associations between residual or lingering lung lesions and differential metabolites were found in the recovered COVID-19 patients, but were not observed in the HC. For example, in the RC patients, PC, homotyrosine, lactoylglutathione,

indolelactate, cyclic AMP, ACN 8:0, maleate and citrate were strongly correlated with CT findings. In the RM patients, 2-hydroxyvalerate, 2-hydroxyisobutyric acid (HIBA), etiocholanolone sulfate (Eti-S), guanine, cystine, and threonine bore intimate relationship with CT findings (Figure 5B).

Blood routine and inflammation

For the inflammation-related clinical indicators, such as Mono, WBC, Lymp, had significant associations with amino acids, such as tyrosine, asparagine, taurine, or organic acids of succinate, hippurate, anthranilate, or lipid species of PE, PC, in the HC, but such associations were not found in the recovered COVID-19 patients. Nonetheless, phenol sulphate, choline, carnitien, glutamine and pyroglutamate were positively associated with CRP (Figure 5C).

Coagulation system

Many correlations between the coagulation function and differential metabolites in the HC were not found in the recovered COVID-19 patients. For example, the level of amino acids, such as leucine, homothreonine, and methionine, 5-hydroxytryptophan, betaine, and phenylalanine, organic acids of anthranilate, abscisate, pantothenate, and maleate had obvious positive correlations to the level of APTT, INR, platelet, FIB, INR or PT (Figure 5D).

Liver function

The liver function indicators of γ-GT, ALT, AST, LDH bore complex relationships with multiple differential metabolites, especially in the HC (Figure 5E). For example, the lipid species (PE, PC), bile acids (GCA, GCDCS, or GUDCA), and amino acids (such as aspartate, phenylalanine, taurine, homotyrosine, methionine) were remarkably related with the level of ALT, AST, γ-GT, or LDH in the HC (Figure 5E). On the other hand, no such associations were found in the RM and RC patients. Moreover, the relationships between 5-hydroxytryptopane and ALT, and between ACN 5:0 and AST, were reversed in the HC and recovered COVID-19 patients.

Heart function

In terms of the heart function, many differential metabolites bore strong relationship with the level of α-HBDH and CK in the health controls, whereas such correlations disappeared in recovered COVID-19 patients. For example, PE, PC and PI were remarkably positively related with the level of CK in the HC, while leucine, Eti-S, ACN 5:0, ACN 3:0, succinate, cyclic AMP, 3-methylxanthine were remarkably associated with the level of α-HBDH in the HC (Figure 5F). Additionally, the level of chlorotyrosine, GCA, hippurate, IAA, MI had unique relationship with the level of CK-MB in the RC patients (Figure 5F).

Kidney function

Figure 5E shows that the level of kidney function variously bore unique relationships with differential metabolites in the recovered COVID-19 patients. For example, the level of glutamine, pyroglutamate, methylhistamine, acylcarnitines of ACN 8:0, ACN 12:1, free carnitine, organic acids of citrate, aconitate, phenol-S, dihydroxymandelate were positively correlated with the level of uric acid (UA), BUN, or creatinine (Cre) (Figure 5G).

Metabolites, as the downstream products of genes and proteins, are implicated in a wide array of biological processes, and play key roles in the homeostasis of biological system. [5] PCs, bile acids and amino acids are important biomolecules that are involved in the regulation of energy metabolism, inflammation, cell proliferation, invasion and apoptosis, and the disordered metabolism of the metabolites have been reported in many diseases. [19-21] Consistently, these metabolites had close relationships with clinical indexes of liver and heart functions, coagulation and inflammation in the HC, indicating they play pivotal roles during these physiological processes. However, these relationships were not observed in the recovered COVID-19 patients, suggesting that the status of these recovered COVID-19 patients may not restore to the level of the HC, even their clinical indicators are shown to be in normal range.

4 Changes in differential metabolites and clinical indexes changes in RC recovered patients are indicative of potential new damage

Notably, the WBC and neutrophils were decreased in the RC patients, which were not different, in the infection period, from HC. The relationships with these two indexes and amino acids, indoles and its derivatives, and organic acids were weak in the RC (Figure 5C). Previous studies revealed that the SARS-CoV-2 may inflict a systemic attack, thereby damaging kidney or lymph nodes, especially in the RC patients. Therefore, these relationships between novel abnormal clinical indexes and differential metabolites in the recovered COVID-19 patients might be present right from the viral attacks during the infection, suggesting that damages are ongoing in the recovered COVID-19 patients.

The UA level was lower in the RC patients at admission, whereas it was higher in the RC patients when compared with HC. Correlation analysis revealed that the increased level of UA was obviously correlated with the levels of critic acid, aconitate, amino acids of methylhistamine, pyroglutamate, glutamine, carnitine, ACN 12:1, methoxyindoleacetate, and cyclic AMP in TCA cycle (Figure 5G).

Discussion

Although COVID-19 survivors worldwide are gradually recovering from mild or severe COVID-19 infection, it remains unclear whether they have fully recovered from severe complications and whether new complications would develop in future after discharge. As we know it, COVID-19 can lead to multi-system damage, and small-molecule metabolites, as the downstream products of genes and proteins are closely associated with the phenotypes and can sensitively reflect slight changes in biological states and have been used in the studies that screen biomarkers of COVID-19. However, few studies focused on the alterations in plasma metabolite profiles in recovered COVID-19 patients. Therefore, our study aimed to profile the plasma metabolites in asymptomatic, moderate, and severe and critical COVID-19 patients 3 months after discharge and provide insights into the recovery from COVID-19. Our results demonstrated that the plasma metabolite profiles in recovered COVID-19 patients were still obviously different from that in HC even 3 months after discharge. This was especially true of the RM and RC patients. Pathway analysis revealed that these metabolic alterations in recovered patients principally involved amino acids, purine, glycerophospholipid metabolism, citrate cycle (TCA cycle), and glyoxylate and dicarboxylate metabolism. Additionally, these alterations bore close relationship with the pulmonary, hepatic, renal, microbial, energetic metabolism and inflammation.

Changes in biochemical, inflammatory indicators and chest CT abnormalities might be found at admission in asymptomatic patients (accounting for a small proportion of total COVID-19 patients). There were no significant differences or there existed only slight differences in clinical parameters between these patients and HC. [21] However, moderate, at admission, severe and critical COVID-19 patients exhibited abnormalities in clinical parameters related to different organs and systems as compared to HC (Table 1). Clinical examinations, including chest CT, suggested that RA patients recovered well but RM and RC patients still had abnormalities in some way as compared with HC (Table 1). These results indicated that there was a significant difference between RA and RM or RC patients and the difference dictated prognosis. Since COVID-19 patients presented with different disease states at admission and eventually had various outcomes, [22] further studies are warranted to evaluate any changes in these recovered patients.

This study showed that the alterations in plasma metabolite profiles in RA, RM and RC patients progressed gradually as compared with HC (Figure 3). Changes in plasma metabolites and clinical indexes in RA patients were similar to those in HC, indicating that RA patients was satisfactory 3 months after discharge. The metabolic disorders in the RM and RC patients mainly implicated amino acids, bile acids, organic acids, and lipids of PC, PE, among others (Figure 4, Table S1). We found that some metabolic abnormalities were present even at the time of SARS-CoV-2 infection. For instance, previous studies revealed that COVID-19 patients had metabolic abnormalities in tricarboxylic acid (TCA) cycle, purine and lipid metabolism. [11-13] Our study showed that these pathways remained disturbed in the recovered COVID-19 patients when compared with the HC, especially in the RC patients. This finding suggested that metabolic abnormalities in COVID-19 patients failed to fully return to normal even 3 months after discharge from hospital.

We also found some new metabolic disorders in convalescent phase, and these disorders were more related to microbial metabolism in the RC patients, such as decreased indole derivatives of indoleacetate (IAA), indolelactate, indole-3-carboxylate, bile acids of GCA, GUDCA (Figure 4A, Figure 6). Intestinal microbiota in patients with active SARS-CoV-2 GI infection was characterized by enrichment of opportunistic pathogens, loss of salutary bacteria and increased functional capacity for related metabolite metabolism. [23,24] Consistently, our study suggested that the SARS-CoV-2 may upset the balance of intestinal flora metabolism, and further aggravate abnormal metabolism in the recovered COVID-19 patients. Indole and indole derivatives are yielded from tryptophan by bacteria in the colonic lumen. Microbiota-derived indoles and metabolites are related to mucosal integrity and protection from inflammation. Indoleacetate, one of tryptophan catabolites, is known to affect intestinal permeability and host immunity. [25] Reduced tryptophan-related indole derivatives are indicative of the loss of gut microbiota homeostasis. Primary bile acids are mainly produced in the liver, and further metabolized by the gut microbiota, [26,27] and its metabolism by bacteria plays an important role in the maintenance of intestinal barrier. [28] Disordered metabolism of bile acids in recovered COVID-19 patients might suggest that the intestinal barrier has not been fully repaired. Totally, the abnormal intestinal flora metabolism prompted us that more attention should be paid to the nutritional status of COVID-19 patients and restoration of metabolic balance of gut microbotia in order to promote the recovery of the patients.

Lung is one of the most-attacked organs during the SARS-CoV-2 infection and many COVID-19 patients present pulmonary lesions on CT. In our study, we found the CT findings of RM and RC patients were still different from those of HC: such as greater PLV, PGV, PCV. Our correction analysis revealed that the level of many altered metabolites bore a unique association with the level of PLV, PGV, PCV. These metabolites included, in the RC patients, homotyrosine, indolelactate, cyclic AMP, ACN 8:0, citrate, aconitate and, in the RM patients, 2-hydroxyvalerate, 2-hydroxyisobutyrate, Eti-S, threonine (Figure 5B). Except the infection of SARS-CoV-2, microbial coinfection was very common, including various viruses, bacteria, and fungi, which not only rendered the diagnosis and treatment of COVID-19 difficult, but also put patients on the risk of unfavorable clinical outcomes. [29,30] Homotyrosine has been reported to be associated with the fungal infection and sulfated homotyrosine echinocandin variants are essential to pathogenicity of some fungi. [31] Indolelactate is one of the bacterial tryptophan metabolites[32] which have been reported to be related to colon cancer, serving as promoters of the disease. [33] Homotyrosine was downregulated while indolelactate was upregulated in recovered COVID-19 patients, suggesting that the disorder caused by microbial coinfection during COVID-19 infection may not disappear in the COVID-19 patients even 3 months after discharge. Cell wall ribitol polymer from Gram-positive organisms can mediate inflammation and cause dysfunction

of pulmonary endothelial cells. [34] In our study, ribitol level was found to be increased in recovered COVID-19 patients, which indicated that the lung inflammation still existed in these recovered COVID-19 patients. Citrate can induce substantial airway constriction and increase in airway responsiveness. [35] The upregulated citrate in recovered COVID-19 patients indicated that the patients' airway was still very sensitive. Cyclic AMP is an important signaling molecule and was increased in recovered COVID-19 patients. The elevated cyclic AMP concentration can reduce airway inflammation and relieve pulmonary edema, [36,37] which suggested that the organ was trying to repair previous damage. The disorders of the lung-function-related metabolites demonstrated that SARS-CoV-2 infection exerted a long-term effect on lungs. Although the recovered COVID-19 patients may present no symptoms subjectively, it is imperative for them to monitor their lung function regularly and identify any abnormalities in time.

We also found the levels of some clinical indexes related to liver (ALP) and heart (CK-MB, α-HBDH) in the recovered COVID-19 patients were still different from those in the HC. Surprisingly, the level of many differential metabolites, including lipid species of PE, PC, bile acids, and amino acids bore strong relationship with the level of γ-GT, ALP, AST, and α-HBDH in the HC, whereas no such associations were observed in the recovered COVID-19 patients (Figure 5E, F). PCs, bile acids, and amino acids are important biomolecules, and play vital roles in the proliferation, invasion, cell apoptosis and inflammation, and their abnormal metabolism has been reportedly related to many diseases. [19,20,38] Liver is one of the major organs that metabolize amino acids, PCs and bile acids. Consistently, our data illustrated that these metabolites were closely related to the functions of liver and heart and help maintain the biological homeostasis in the HC. Dysregulation of these metabolites are reported in many liver- or heart-related diseases. [19,39] COVID-19 patients at admission showed liver function abnormalities and failed to fully recover even after discharge. This was especially true of the severe and critical COVID-19 patients.[8,9,32] Therefore, we hypothesize that these metabolic disruptions in the recovered COVID-19 patients might also result from damages caused by COVID-19 viruses. The elevation of bile acid derivatives, such as chenodeoxycholic acid (CDCA), glycochenodeoxycholate-3-sulfate (GCDCS) in the plasma of recovered patients, compared with HC, may indicate hepatic detoxification function was impaired and biliary ducts were injured. [40] Analysis of metabolomic data revealed that serum lipids were reduced in COVID-19 infected patients. [13] Consistently, the lowered lipids of PCs and PEs might result from the SARS-CoV-2 infection. In our study, various lipids were still down-regulated in the recovered patients. Collectively, these findings suggested that the liver sustained persistent damage in COVID-19 patients.

Kidney injury is a common complication of COVID-19[41] and leads to the accumulation of metabolites that are toxic to other systems. Our study showed that the levels of creatinine and UA, two renal function indicators, were still higher in RM or RC patients than in the HC (Table 1), indicating that the renal injury might not be completely reversed. To further investigate the underlying mechanism of these abnormalities, association analysis was performed. It is noteworthy that many altered metabolites showed unique association with the indicators of renal functions in the recovered COVID-19 patients, such as the conspicuous positive relationships between the level of citrate, aconitate, pantothenate, and the level of clinical indexes of UA and/or creatinine (Figure 5G). Citrate, and aconitate can directly enter the TCA cycle for the energy production in the mitochondria. Previous studies reported that the metabolism of TCA cycle in COVID-19 patients is disrupted. [11,12] With chronic and diabetic kidney diseases, TCA cycle was disrupted, which may be caused by mitochondrial dysfunction. [42,43] In this study, the increased level of citrate, and aconitate in the recovered COVID-19 patients indicated their mitochondrial function may not restore to normal. Pantothenate, the precursor of coenzyme A (CoA), can slow cell injury and apoptosis and promote cell repair by increasing glutathione biosynthesis, or resistance to lipid peroxidation by forming CoA. [44,45] A previous study revealed that the decreased pantothenate in the acute renal injury might reduce antioxidant capacity of kidney. [46] In our study, the level of pantothenate was higher in RC patients than in HC, indicating that the renal antioxidant capacity was increased and more pantothenate was recruited to repair virus-caused damage. Furthermore, both of clinical test and metabolomic analysis exhibited that the UA level was higher in the RC patients than in HC. UA, a purine derivative, is the final oxidation product of purine metabolism. Interestingly, we found that many metabolites, such as inosine, hypoxanthine, guanine, and cyclic AMP, in the purine metabolism were decreased in the recovered COVID-19 patients (Figure 6). Therefore, we theorize that the xanthine oxidase, an enzyme for uric acid production, was highly expressed and/or its renal excretion was obstructed in the RC patients. The assumption needs further study. Since UA is a uremic toxin identified by the European Uremic Toxin Working Group, [45] we recommend that recovered COVID-19 patients be tested for renal function in future.

WBC and neutrophils, two clinical measures, were decreased in the RC patients but were similar to these of HC. As we know it, neutrophils, the common innate immune cells, can activate the host defense during infection and eliminate most microorganisms that infect humans. [47] A subgroup patient infected by virus, such as influenza, hepatitis, varicella, measles, rubella, Epstein-Barr virus etc may have reduced neutrophils, but such reduction is mostly self-limiting and sometimes persists. One of the possible mechanisms might be that the lowered bone marrow granulocyte reserve leads to the neutrophil reduction. [48] Although the level of neutrophils is relatively low, the patients are predisposed to infection, [47] overall levels remained within the normal range. Therefore, further monitoring of bone marrow hematopoiesis, by bone marrow puncture, was not necessary. The number of neutrophils should be monitored on regular basis.

Other organs may also be affected in recovered COVID-19 patients. Taurine is an essential sulfur-containing semi-essential amino acid which plays a crucial physiological role. [49] In cardiovascular diseases, taurine can not only lower blood pressure and improves vascular function in prehypertensive status, [50] but also reduce the potential of atherogenesis in animal models. [51,52] Cardiomyocyte atrophy and cardiac dysfunction

were reportedly caused by taurine depletion. [53] Moreover, taurine depletion can lead to malfunction of pancreatic β cells, which may reduce the plasma insulin levels. [54] In our study, taurine was reduced in the recovered COVID-19 patients, and the relationship between taurine and α-HBDH was reversed from a positive correlation in the HC to a negative one in the RM patients (Figure 5F), indicating that SARS-CoV-2 infection impairs cardiovascular function. Choline and glutamine were positively correlated with CRP level. Glutamine is essential for T cell differentiation and macrophage polarization, and the increased glutamine can elevate oxygen consumption in effector T cells and promote T cell activation. [55] The level of glutamine was elevated and was positively correlated with the level of CRP in the recovered COVID-19 patients, suggesting that inflammation worsens in the recovered COVID-19 patients. Choline is an essential nutrient and is required for many important physiological functions, including methyl group metabolism, the structural integrity and signaling of cells. [56,57] Choline was up-regulated in recovered COVID-19 patients. Elevated concentration of plasma choline has been reported to be associated with cardiometabolic risk factors and history of cardiovascular disease in elderly subjects. [58] The findings are consistent with the recent studies that older COVID-19 patients with comorbidities, especially cardiovascular diseases, go through severe illness more easily. [59] Meanwhile, high choline intake was associated with increased cardiometabolic mortality in racially diverse populations and the choline-mortality association appeared stronger among individuals with existing cardiometabolic disease. [60] Additionally, metabolic alterations of choline are related to a higher risk for type 2 diabetes (T2D) due to impaired insulin sensitivity. [61] T2D is considered to be a major comorbidity of COVID-19. [62] Plasma phenylalanine levels were observed to be deceased in patients with cardiovascular disease (CVD) that occurred after development of atherosclerosis in the coronary or carotid arteries. [63] Metabolic disturbances of phenylalanine are considered to be associated with the poor prognosis of heart failure. [39] Phenylalanine was down-regulated in recovered COVID-19 patients, which indicate that the recovered COVID-19 patients might potentially develop some cardiac abnormalities in future.

Limitations of Study

In this study, laboratory, chest CT findings and metabolic changes in plasma were examined in patients without underlying diseases. However, this study had several limitations. Firstly, this is a single-center prospective study with a relatively small sample size, especially in RA group. Secondly, considering that RA patients in this study were detected by screening for SARS-CoV-2 antibodies, it's hard to determine when they had recovered. Thirdly, blood routine test, liver and kidney function, and chest CT findings were not sensitive indicators of the organ injury presented by metabolomics. Future studies that include large-sized cohort and using more sensitive measures are warranted.

Methods

Study Participants and Sample Collection

Wuhan Union Hospital was mandatorily designated to take care of moderate, severe and critical COVID-19 patients. This prospective study enrolled a total of 78 COVID-19 adult patients without underlying diseases before admission, including 34 RM patients and 44 RC patients who had been discharged from Wuhan Union Hospital 3 months ago. Currently, 18 RA and 39 HC subjects now live in Wuhan. All participants were negative for SARS-CoV-2 nucleic acid as confirmed by real-time polymerase chain reaction at the time of inclusion. There were no statistically significant differences in baseline characteristics, such as age, sex, and body mass index (BMI) between HC and different recovered groups (RA, RM and RC groups). COVID-19 patients were diagnosed and stratified at admission according to the New Coronavirus Pneumonia Prevention and Control Program (the 7th edition) released by the National Health Commission of China. In details, moderate cases had fever or respiratory symptoms with possibly characteristic imaging findings of pneumonia. Severely-ill cases were diagnosed if one of the following was present: (1) RR $\geq$ 30/min at rest; (2) oxygen saturation below 93% at rest; (3) $PaO_2/FiO_2 \leq 300$ mmHg; (4) over 50% deterioration of imaging findings over a period of 24-48 hours. Critical cases were diagnosed if any of the following was met: (1) respiratory failure and the need for mechanical ventilation; (2) development of shock; (3) failure of other vital organs and the need of intensive care. Healthy control and asymptomatic carriers were from the health checkup department. healthy control were the adults who tested negative for IgG and IgM of SARS-CoV-2 and had no diseases at the same period while the asymptomatic carrier was the adults positive for IgG but negative for IgM of SARS-CoV-2, without symptoms and underlying diseases at the same period.

All participants underwent blood tests, including complete blood count, coagulation profile, renal and liver function, creatine kinase and chest computerized tomography (CT). Simultaneously, we collected their peripheral blood for subsequent untargeted metabolomic determination. Baseline characteristics and laboratory findings in recovered COVID-19 patients and HC are summarized in Table 1. Clinical and laboratory data of hospitalized moderate, severely- and critically-ill patients were extracted from electronic medical records and are also given in Table 1. The clinical data of the patients and HC were collected and checked independently by three physicians (Siwei Song, Xueyun Tan and Hui Xia). This study was conducted in line with the Declaration of Helsinki. The institutional ethics committees of Wuhan Union Hospital (No. 0036) reviewed and approved this study protocol. And this study was registered on the Clinical Trials website (NCT04283396). All enrolled patients signed an informed consent.

Chest CT and artificial intelligence (AI)-based quantification of CT images

Chest CT was performed in these subjects by using a 126-slice CT scanner (Ingenuity Core 128, Philips) with standard imaging protocols as follows: CT tube voltage 120KV and tube current 80-250 mA, CT rotation time 0.3-0.75 second, CT detector collimation 64*0.6 mm and image

matrix 512*512，pitch 1.5; section thickness 1.0 mm.

Radiological findings, including GGO, fibrous stripe, thickening of the adjacent pleura, bronchovesicular bundle distortion and small pleural effusion, were collected and estimated by two imaging specialists with over 10-year experience (Lian Yang and Fan Yang). The GGO was defined as a hazy area of increased attenuation without obscuration of the underlying vasculature. [64] Fibrous stripe was defined as a linear opacity with fine fibrosis and was usually associated with distortion of the lung architecture. [64] Thickening of the adjacent pleura was defined as thickening of the adjacent fissural or peripheral pleura. [65] Bronchovascular bundle distortion/architectural distortion was defined as distorted appearance of lung anatomy characterized by abnormal displacement of bronchi, vessels, fissures, or septa caused by diffuse or localized lung disease, particularly interstitial fibrosis. [64]

In addition, an artificial intelligence (AI)-based quantitative evaluation system (YITU Healthcare Technology, China) was used to calculate the pneumonia lesions by analyzing CT values. This AI system[18] was developed and validated in COVID-19 patients and showed preferable pneumonia lesion segmentation. In brief, lung segmentation using deep learning-based approach allows a machine to be fed raw data of CT scans and to automatically discover the location, outline and density of region-of-interest (ROI) in each CT image. The results were also rechecked and corrected by the aforementioned two imaging specialists. According to the above-mentioned results, the proportion of ROI was calculated. By thresholding on CT values in the pneumonia lesions, two quantitative features were computed, i.e., the percentages of GGO volume with ranges of ≥-700 hounsfield unit (HU) and <-500 HU, and consolidation with ≥-200 HU and <60 HU. AI-derived CT features corresponded to percentages of GGO volume (PGV), consolidation volume (PCV), and both (equal to 100 × lesions volume/bilateral lung volume) (PLV).

Plasma Collection and Metabolite Extraction

All healthy individuals and recovered patients had been told to fast and to restrict fluid intake for 12 hours and not take any drugs or dietary supplements for 48 hours before the blood collection. Venous blood (10 mL) was collected in the morning into heparin sodium anticoagulant tube, centrifuged at 2000 rpm for 10 minutes at 4°C to extract plasma. All plasma samples were stored at –80°C until analysis.

The plasma samples were thawed at 4 °C and vortexed for 30 seconds. 300 μL of methanol (precooling at -20°C) were added into the 100 μL of sample/reagent blank (pure water), then vortexed for 1 min and extracted at -20 °C. After 20 mins, the mixture was vortexed for 1 min and centrifuged at 10000 rpm for 10 min at 4 °C. 260 μL of supernatant was transferred to the new centrifuge tube and dried under stream of nitrogen. The dried contents were reconstituted in 100 μL ultrapure water and vortexed for 1 min, and centrifuged at 10000 rpm for 10 min at 4 °C. Afterwards, all supernatant was taken for LC-MS analysis.

Untargeted LC-MS-based Metabolomic analysis

Prepared plasma supernatant was detected for metabolites by using ultra-high performance liquid chromatography (Ultimate 3000, hermo Scientific, USA) in series on the Q Exactive high-resolution mass spectrometry (HRM) system (Thermo Scientific, USA). ACQUITY UPLC HSS T3 column (1.8 μm, 100mm×2.1mm ID) (Waters, USA) was used for chromatographic separation. Data were acquired by scanning positive and negative ions separately. 2 μL of samples was injected into the LC-MS system for each ion mode detection. The column temperature was maintained at 35°C and the flow rate was set at 0.35 mL/min. The mobile phase in the positive ion mode was made of an aqueous solution containing 0.1% formic acid (Mobile Phase A) and 100% methanol containing 0.1% formic acid (Mobile Phase B). The mobile phase in the negative ion mode was made of an aqueous solution containing 10 mM ammonium formate (Mobile Phase A) and 95% methanol containing 10 mM ammonium formate (Mobile Phase B). The chromatographic gradient was 0 min at 10% B, 1 min at 10% B, 13 min at 98% B, 18 min at 98% B, 18.5 min at 10% B, 20 min at 10% B for both ion modes. Metabolic data were obtained by both Q Exactive full scan and MS/MS data using Data-dependent Acquisition method. The collision energy for positive ions was set at 3.8kV and negative ions was at 3.2kV. Raw data were converted into a common (ABF) format by AnalysisBase File Converter.

Quantification and statistical analysis

Peak alignment of the acquired raw data was performed using MSDIAL software package (http://prime.psc.riken.jp/compms/msdial/main.html). After removing missing values, [66] the signal drifts of the remaining matched peak ions were calibrated by global linear regression (Goreg) to minimize the effect of instability of data. [19,67] Metabolites were identified by the online research of HMDB (https://hmdb.ca/) and MSBank (http://www.massbank.jp/) and mzCloud (Thermo Scientific, USA) of MS1 and MS2, or on the basis of our previous studies. [19,68] Partial least square-discriminate analysis (PLS-DA) was conducted using SIMCA-P software (version 11.0; Umetrics). Wilcoxon Mann-Whitney test with Benjamini-Hochberg-based false discovery rate (FDR) correction was utilized to define the statistical significance of metabolites by Multi Experiment Viewer software (MeV, version 4.7.4), with $P < 0.05$ and $FDR < 0.05$ taken as statistically significant. Pearson correlation analysis among the clinical parameters and differential metabolites was carried out by employing SPSS software (version 18.0.0), and its network was displayed by using Cytoscape software (version 3.7.1). Metabolite pathway analysis was conducted by employing the online software of Metaboanalyst (https://www.metaboanalyst.ca/MetaboAnalyst/).

Declarations

Acknowledgements

The authors sincerely are grateful to all the patients, individuals and investigators who participated in this study. We thank the support form Wuhan Anachro Technologies Inc. on metabonomics, and from Wuhan YITU Company on artificial intelligence. This work was supported by the National Natural Science Foundation of China (82041018; 81802113), Major Projects of the National Science and Technology (2019ZX09301001), Ministry of Science and Technology of the People's Republic of China (2020YFC0844300), and the Fundamental Research Funds for the Central Universities, HUST (2020kfyXGYJ011).

Author contributions

YJ designed the study and responsible for the integrity of the work as a whole. JX, LY, QC, YM, FY, LY, YL and GM collected the epidemiological and clinical data. SS, XT, HX, SZ and PM summarized all date. SW, PL, LY, ZW and YD analyzed the date. JX and LY interpreted all date. SW, PL, SS, XT, HX, SZ and PM drafted the initial draft. All authors participated in the discussion of initial draft and propounded constructive suggestions for revision. SW, PL and SS revised the final manuscript. All authors reviewed and approved the final version.

Declaration interest

The authors declare no competing interests.

References

1 Fang, Y., Zhou, J., Ding, X., Ling, G. & Yu, S. Pulmonary fibrosis in critical ill patients recovered from COVID-19 pneumonia: Preliminary experience. *Am J Emerg Med*, doi:10.1016/j.ajem.2020.05.120 (2020).

2 Puntmann, V. O. *et al.* Outcomes of Cardiovascular Magnetic Resonance Imaging in Patients Recently Recovered From Coronavirus Disease 2019 (COVID-19). *JAMA cardiology*, doi:10.1001/jamacardio.2020.3557 (2020).

3 Huang, L. *et al.* Cardiac Involvement in Patients Recovered From COVID-2019 Identified Using Magnetic Resonance Imaging. *JACC. Cardiovascular imaging*, doi:10.1016/j.jcmg.2020.05.004 (2020).

4 Li, J. *et al.* Olfactory Dysfunction in Recovered Coronavirus Disease 2019 (COVID-19) Patients. *Movement disorders : official journal of the Movement Disorder Society* **35**, 1100-1101, doi:10.1002/mds.28172 (2020).

5 Ayres, J. S. A metabolic handbook for the COVID-19 pandemic. *Nature metabolism* **2**, 572-585, doi:10.1038/s42255-020-0237-2 (2020).

6 Wu, Q. *et al.* Altered Lipid Metabolism in Recovered SARS Patients Twelve Years after Infection. *Scientific reports* **7**, 9110, doi:10.1038/s41598-017-09536-z (2017).

7 Banoei, M. M. *et al.* Plasma metabolomics for the diagnosis and prognosis of H1N1 influenza pneumonia. *Critical care (London, England)* **21**, 97, doi:10.1186/s13054-017-1672-7 (2017).

8 Fujiogi, M. *et al.* Respiratory viruses are associated with serum metabolome among infants hospitalized for bronchiolitis: A multicenter study. *Pediatric allergy and immunology : official publication of the European Society of Pediatric Allergy and Immunology*, doi:10.1111/pai.13296 (2020).

9 Eisfeld, A. J. *et al.* Multi-platform 'Omics Analysis of Human Ebola Virus Disease Pathogenesis. *Cell host & microbe* **22**, 817-829.e818, doi:10.1016/j.chom.2017.10.011 (2017).

10 Cui, L. *et al.* Serum metabolome changes in adult patients with severe dengue in the critical and recovery phases of dengue infection. *PLoS neglected tropical diseases* **12**, e0006217, doi:10.1371/journal.pntd.0006217 (2018).

11 Song, J. W. *et al.* Omics-Driven Systems Interrogation of Metabolic Dysregulation in COVID-19 Pathogenesis. *Cell metabolism* **32**, 188-202.e185, doi:10.1016/j.cmet.2020.06.016 (2020).

12 Wu, D. *et al.* Plasma metabolomic and lipidomic alterations associated with COVID-19. *National Science Review* **7**, 1157-1168, doi:10.1093/nsr/nwaa086 (2020).

13 Shen, B. *et al.* Proteomic and Metabolomic Characterization of COVID-19 Patient Sera. *Cell* **182**, 59-72.e15, doi:10.1016/j.cell.2020.05.032 (2020).

14 Jiang, H. *et al.* SARS-CoV-2 proteome microarray for global profiling of COVID-19 specific IgG and IgM responses. *Nature communications* **11**, 3581, doi:10.1038/s41467-020-17488-8 (2020).

15 Wang, S. *et al.* Fasting blood glucose at admission is an independent predictor for 28-day mortality in patients with COVID-19 without previous diagnosis of diabetes: a multi-centre retrospective study. *Diabetologia* **63**, 2102-2111, doi:10.1007/s00125-020-05209-1 (2020).

16 Sun, Y. *et al.* Characteristics and prognostic factors of disease severity in patients with COVID-19: The Beijing experience. *Journal of autoimmunity* **112**, 102473, doi:10.1016/j.jaut.2020.102473 (2020).

17 Zhang, J., Lee, K., Ang, L., Leo, Y. & Young, B. Risk Factors of Severe Disease and Efficacy of Treatment in Patients Infected with COVID-19: A Systematic Review, Meta-Analysis and Meta-Regression Analysis. *Clinical infectious diseases : an official publication of the Infectious Diseases Society of America*, doi:10.1093/cid/ciaa576 (2020).

18 Liu, F. *et al.* CT quantification of pneumonia lesions in early days predicts progression to severe illness in a cohort of COVID-19 patients. *Theranostics* **10**, 5613-5622, doi:10.7150/thno.45985 (2020).

19 Luo, P. *et al.* A Large-scale, multicenter serum metabolite biomarker identification study for the early detection of hepatocellular carcinoma. *Hepatology (Baltimore, Md.)* **67**, 662-675, doi:10.1002/hep.29561 (2018).

20 Maddocks, O. D. *et al.* Serine starvation induces stress and p53-dependent metabolic remodelling in cancer cells. *Nature* **493**, 542-546, doi:10.1038/nature11743 (2013).

21 Long, Q. X. *et al.* Clinical and immunological assessment of asymptomatic SARS-CoV-2 infections. *Nature medicine* **26**, 1200-1204, doi:10.1038/s41591-020-0965-6 (2020).

22 Wu, Z. & McGoogan, J. M. Characteristics of and Important Lessons From the Coronavirus Disease 2019 (COVID-19) Outbreak in China: Summary of a Report of 72 314 Cases From the Chinese Center for Disease Control and Prevention. *Jama* **323**, 1239-1242, doi:10.1001/jama.2020.2648 (2020).

23 Zuo, T. *et al.* Depicting SARS-CoV-2 faecal viral activity in association with gut microbiota composition in patients with COVID-19. *Gut*, doi:10.1136/gutjnl-2020-322294 (2020).

24 Gu, S. *et al.* Alterations of the Gut Microbiota in Patients with COVID-19 or H1N1 Influenza. *Clinical infectious diseases : an official publication of the Infectious Diseases Society of America*, doi:10.1093/cid/ciaa709 (2020).

25 Agus, A., Planchais, J. & Sokol, H. Gut Microbiota Regulation of Tryptophan Metabolism in Health and Disease. *Cell host & microbe* **23**, 716-724, doi:10.1016/j.chom.2018.05.003 (2018).

26 Ridlon, J., Harris, S., Bhowmik, S., Kang, D. & Hylemon, P. Consequences of bile salt biotransformations by intestinal bacteria. *Gut microbes* **7**, 22-39, doi:10.1080/19490976.2015.1127483 (2016).

27 Wahlström, A., Sayin, S., Marschall, H. & Bäckhed, F. Intestinal Crosstalk between Bile Acids and Microbiota and Its Impact on Host Metabolism. *Cell metabolism* **24**, 41-50, doi:10.1016/j.cmet.2016.05.005 (2016).

28 Thomas, C., Pellicciari, R., Pruzanski, M., Auwerx, J. & Schoonjans, K. Targeting bile-acid signalling for metabolic diseases. *Nature reviews. Drug discovery* **7**, 678-693, doi:10.1038/nrd2619 (2008).

29 Chen, X. *et al.* The microbial coinfection in COVID-19. *Applied microbiology and biotechnology* **104**, 7777-7785, doi:10.1007/s00253-020-10814-6 (2020).

30 Zhang, G. *et al.* Clinical features and short-term outcomes of 221 patients with COVID-19 in Wuhan, China. *Journal of clinical virology : the official publication of the Pan American Society for Clinical Virology* **127**, 104364, doi:10.1016/j.jcv.2020.104364 (2020).

31 Wingfield, B. D. *et al.* IMA Genome-F 9: Draft genome sequence of Annulohypoxylon stygium, Aspergillus mulundensis, Berkeleyomyces basicola (syn. Thielaviopsis basicola), Ceratocystis smalleyi, two Cercospora beticola strains, Coleophoma cylindrospora, Fusarium fracticaudum, Phialophora cf. hyalina, and Morchella septimelata. *IMA fungus* **9**, 199-223, doi:10.5598/imafungus.2018.09.01.13 (2018).

32 Gao, J. *et al.* Impact of the Gut Microbiota on Intestinal Immunity Mediated by Tryptophan Metabolism. *Frontiers in cellular and infection microbiology* **8**, 13, doi:10.3389/fcimb.2018.00013 (2018).

33 Zuccato, E. *et al.* Role of bile acids and metabolic activity of colonic bacteria in increased risk of colon cancer after cholecystectomy. *Digestive diseases and sciences* **38**, 514-519, doi:10.1007/bf01316508 (1993).

34 Pai, A. B. *et al.* Lipoteichoic acid from Staphylococcus aureus induces lung endothelial cell barrier dysfunction: role of reactive oxygen and nitrogen species. *PloS one* **7**, e49209, doi:10.1371/journal.pone.0049209 (2012).

35 Lai, Y. L., Chiou, W. Y., Lu, F. J. & Chiang, L. Y. Roles of oxygen radicals and elastase in citric acid-induced airway constriction of guinea-pigs. *British journal of pharmacology* **126**, 778-784, doi:10.1038/sj.bjp.0702352 (1999).

36 Chen, Y. F. *et al.* Exchange protein directly activated by cAMP (Epac) protects against airway inflammation and airway remodeling in asthmatic mice. *Respiratory research* **20**, 285, doi:10.1186/s12931-019-1260-2 (2019).

37 Wang, M. *et al.* Adenosine A(2B) receptor activation stimulates alveolar fluid clearance through alveolar epithelial sodium channel via cAMP pathway in endotoxin-induced lung injury. *American journal of physiology. Lung cellular and molecular physiology* **318**, L787-l800, doi:10.1152/ajplung.00195.2019 (2020).

38 Xicoy, H., Wieringa, B. & Martens, G. J. M. The Role of Lipids in Parkinson's Disease. *Cells* **8**, doi:10.3390/cells8010027 (2019).

39 Cheng, M. L. *et al.* Metabolic disturbances identified in plasma are associated with outcomes in patients with heart failure: diagnostic and prognostic value of metabolomics. *Journal of the American College of Cardiology* **65**, 1509-1520, doi:10.1016/j.jacc.2015.02.018 (2015).

40 Rowland, A., Miners, J. & Mackenzie, P. The UDP-glucuronosyltransferases: their role in drug metabolism and detoxification. *The international journal of biochemistry & cell biology* **45**, 1121-1132, doi:10.1016/j.biocel.2013.02.019 (2013).

41 Gabarre, P. *et al.* Acute kidney injury in critically ill patients with COVID-19. *Intensive Care Med* **46**, 1339-1348, doi:10.1007/s00134-020-06153-9 (2020).

42 Hallan, S. *et al.* Metabolomics and Gene Expression Analysis Reveal Down-regulation of the Citric Acid (TCA) Cycle in Non-diabetic CKD Patients. **26**, 68-77, doi:10.1016/j.ebiom.2017.10.027 (2017).

43 Tan, S. *et al.* Complement C5a Induces Renal Injury in Diabetic Kidney Disease by Disrupting Mitochondrial Metabolic Agility. **69**, 83-98, doi:10.2337/db19-0043 (2020).

44 Naquet, P., Kerr, E., Vickers, S. & Leonardi, R. J. P. i. l. r. Regulation of coenzyme A levels by degradation: the 'Ins and Outs'. **78**, 101028, doi:10.1016/j.plipres.2020.101028 (2020).

45 Duranton, F. *et al.* Normal and pathologic concentrations of uremic toxins. **23**, 1258-1270, doi:10.1681/asn.2011121175 (2012).

46 Ping, F. *et al.* Metabolomics Analysis of the Renal Cortex in Rats With Acute Kidney Injury Induced by Sepsis. **6**, 152, doi:10.3389/fmolb.2019.00152 (2019).

47 Netea, M. G. *et al.* Trained Immunity: a Tool for Reducing Susceptibility to and the Severity of SARS-CoV-2 Infection. *Cell* **181**, 969-977, doi:10.1016/j.cell.2020.04.042 (2020).

48 Gibson, C. & Berliner, N. How we evaluate and treat neutropenia in adults. *Blood* **124**, 1251-1258; quiz 1378, doi:10.1182/blood-2014-02-482612 (2014).

49 Jakaria, M. *et al.* Taurine and its analogs in neurological disorders: Focus on therapeutic potential and molecular mechanisms. *Redox biology* **24**, 101223, doi:10.1016/j.redox.2019.101223 (2019).

50 Sun, Q. *et al.* Taurine Supplementation Lowers Blood Pressure and Improves Vascular Function in Prehypertension: Randomized, Double-Blind, Placebo-Controlled Study. *Hypertension (Dallas, Tex. : 1979)* **67**, 541-549, doi:10.1161/hypertensionaha.115.06624 (2016).

51 Murakami, S. *et al.* Prevention of neointima formation by taurine ingestion after carotid balloon injury. *Vascular pharmacology* **53**, 177-184, doi:10.1016/j.vph.2010.07.003 (2010).

52 Zulli, A. *et al.* High dietary taurine reduces apoptosis and atherosclerosis in the left main coronary artery: association with reduced CCAAT/enhancer binding protein homologous protein and total plasma homocysteine but not lipidemia. *Hypertension (Dallas, Tex. : 1979)* **53**, 1017-1022, doi:10.1161/hypertensionaha.109.129924 (2009).

53 Ito, T. *et al.* Taurine depletion caused by knocking out the taurine transporter gene leads to cardiomyopathy with cardiac atrophy. *Journal of molecular and cellular cardiology* **44**, 927-937, doi:10.1016/j.yjmcc.2008.03.001 (2008).

54 L'Amoreaux, W. J. *et al.* Taurine regulates insulin release from pancreatic beta cell lines. *Journal of biomedical science* **17 Suppl 1**, S11, doi:10.1186/1423-0127-17-s1-s11 (2010).

55 Angajala, A. *et al.* Diverse Roles of Mitochondria in Immune Responses: Novel Insights Into Immuno-Metabolism. *Front Immunol* **9**, 1605, doi:10.3389/fimmu.2018.01605 (2018).

56 Zeisel, S. H. Choline: an essential nutrient for humans. *Nutrition (Burbank, Los Angeles County, Calif.)* **16**, 669-671, doi:10.1016/s0899-9007(00)00349-x (2000).

57 Zeisel, S. H. & Blusztajn, J. K. Choline and human nutrition. *Annual review of nutrition* **14**, 269-296, doi:10.1146/annurev.nu.14.070194.001413 (1994).

58 Roe, A. J. *et al.* Choline and its metabolites are differently associated with cardiometabolic risk factors, history of cardiovascular disease, and MRI-documented cerebrovascular disease in older adults. *The American journal of clinical nutrition* **105**, 1283-1290, doi:10.3945/ajcn.116.137158 (2017).

59 Guan, W. J. *et al.* Comorbidity and its impact on 1590 patients with COVID-19 in China: a nationwide analysis. *The European respiratory journal* **55**, doi:10.1183/13993003.00547-2020 (2020).

60 Yang, J. J. *et al.* Associations of choline-related nutrients with cardiometabolic and all-cause mortality: results from 3 prospective cohort studies of blacks, whites, and Chinese. *The American journal of clinical nutrition* **111**, 644-656, doi:10.1093/ajcn/nqz318 (2020).

61 Floegel, A. *et al.* Identification of serum metabolites associated with risk of type 2 diabetes using a targeted metabolomic approach. *Diabetes* **62**, 639-648, doi:10.2337/db12-0495 (2013).

62 Zhu, L. *et al.* Association of Blood Glucose Control and Outcomes in Patients with COVID-19 and Pre-existing Type 2 Diabetes. *Cell metabolism* **31**, 1068-1077.e1063, doi:10.1016/j.cmet.2020.04.021 (2020).

63 Tzoulaki, I. *et al.* Serum metabolic signatures of coronary and carotid atherosclerosis and subsequent cardiovascular disease. *European heart journal* **40**, 2883-2896, doi:10.1093/eurheartj/ehz235 (2019).

64 Hansell, D. M. *et al.* Fleischner Society: glossary of terms for thoracic imaging. *Radiology* **246**, 697-722, doi:10.1148/radiol.2462070712 (2008).

65 Shi, H. *et al.* Radiological findings from 81 patients with COVID-19 pneumonia in Wuhan, China: a descriptive study. *The Lancet Infectious Diseases* **20**, 425-434, doi:10.1016/s1473-3099(20)30086-4 (2020).

66 Smilde, A. K., van der Werf, M. J., Bijlsma, S., van der Werff-van der Vat, B. J. & Jellema, R. H. Fusion of mass spectrometry-based metabolomics data. *Analytical chemistry* **77**, 6729-6736, doi:10.1021/ac051080y (2005).

67 Dunn, W. B. *et al.* Procedures for large-scale metabolic profiling of serum and plasma using gas chromatography and liquid chromatography coupled to mass spectrometry. *Nature protocols* **6**, 1060-1083, doi:10.1038/nprot.2011.335 (2011).

68 Luo, P. *et al.* Metabolic characteristics of large and small extracellular vesicles from pleural effusion reveal biomarker candidates for the diagnosis of tuberculosis and malignancy. *Journal of Extracellular Vesicles* **9**, 1790158, doi:10.1080/20013078.2020.1790158 (2020).

Tables

Table 1. Clinical and laboratory findings of healthy controls and COVID-19 patients.

		COVID-19 patients at admission		Recovered COVID-19 patients		
Variables	HC (N=39)	M (N=34)	C (N=44)	RA (N=18)	RM (N=34)	RC (N=44)
Characteristics						
Age, years	41.00 (32.00, 52.00)	47.50 (42.00, 54.00)	46.50 (38.50, 56.00)	43.50 (38.00,52.00)	47.50 (42.00, 54.00)	46.50 (38.50, 56.00)
Sex						
Female	23 (58.97)	25 (73.53)	20 (45.45)	8(44.44)	25 (73.53)	20 (45.45)
Male	16 (41.03)	9(26.47)	24 (54.55)	10 (55.56)	9 (26.47)	24 (54.55)
BMI, kg/m^2	22.97 (21.23, 25.24)	-	-	24.18 (22.96,25.21)	23.88 (21.88, 26.23)	24.52 (22.72, 26.83)
Laboratory findings						
SARS-CoV-2 nucleic acid test（+）	0(0.00)	0(0.00)	0(0.00)	0(0.00)	0(0.00)	0(0.00)
IgG (+)	0(0.00)	-	-	16 (88.89)	33 (97.06)	42 (97.67)
IgM (+)	0(0.00)	-	-	2 (11.11)	6 (17.65)	9 (20.93)
CRP, mg/L	0.71 (0.41, 1.26)	3.24 (0.10, 6.25) [a]	18.57 (2.82, 32.25) [a]	0.69 (0.08, 1.29)	1.06 (0.16, 1.69) [b]	0.70 (0.35, 1.42) [c]
WBC, $\times 10^9$ per L	5.50 (4.98, 6.43)	5.91 (4.90, 7.02)	5.16 (4.16, 6.43)	5.25 (4.78, 5.72)	5.18 (4.48, 6.08) [b]	5.08 (4.42, 5.75) [a]
RBC, $\times 10^{12}$ per L	4.74 (4.40, 5.21)	4.13 (3.79, 4.44) [a]	4.25 (3.81, 4.71) [a]	4.73 (4.37, 5.21)	4.56 (4.34, 5.01) [b]	4.77 (4.43, 5.22) [c]
Haemoglobin, g/L	146.00 (134.00,162.00)	125.50(120.00, 134.00)[a]	130.50(119.00, 141.00)[a]	151.00(139.00, 162.00)	141.50(138.00,155.00)[b]	146.50(137.50,157.00)[c]
MCV, fl	93.20 (89.70, 95.80)	91.35 (88.50, 95.10)	91.95 (90.05, 94.65)	94.00 (89.70, 96.20)	91.55 (88.60, 95.00)	92.60 (90.30, 95.40)
MCH, pg	31.30 (30.10, 32.70)	30.75 (29.70, 31.70)	30.95 (30.05, 31.90)	31.80 (30.00, 33.00)	31.10 (30.00, 32.10) [b]	31.00 (30.35, 31.85)
MCHC, g/L	336.00(332.00, 343.00)	333.00(327.00, 337.00)[a]	334.00(331.00, 338.00)	340.00(337.00, 345.00)	337.00(333.00,344.00)[b]	334.50(330.00, 339.50)
Platelets, $\times 10^9$ per L	217.00(180.00, 261.00)	225.50(190.00, 260.00)	211.50(165.50, 261.00)	192.50(181.00, 221.00)	210.00(173.00, 254.00)	209.00(181.00, 229.50)
Neutrophils, $\times 10^9$ per L	3.15 (2.81, 3.84)	3.60 (2.75, 4.60)	3.32 (2.40, 4.48)	3.26 (2.69, 3.56)	2.96 (2.53, 3.81) [b]	2.93 (2.44, 3.26) [ac]
Lymphocytes, $\times 10^9$ per L	1.84 (1.45, 2.10)	1.62 (1.36, 2.06)	1.25 (0.88, 1.53) [a]	1.56 (1.26, 2.02)	1.58 (1.46, 1.95)	1.73 (1.37, 2.05) [c]
Monocytes, $\times 10^9$ per L	0.27 (0.23, 0.34)	0.43 (0.32, 0.46) [a]	0.39 (0.29, 0.44) [a]	0.30 (0.21, 0.31)	0.27 (0.23, 0.33) [b]	0.29 (0.20, 0.33) [c]
Eosinophils, $\times 10^9$ per L	0.09 (0.06, 0.17)	0.10 (0.07, 0.20)	0.04 (0.01, 0.10) [a]	0.07 (0.04, 0.10)	0.09 (0.06, 0.13) [b]	0.10 (0.06, 0.14) [c]
Basophils, $\times 10^9$ per L	0.01 (0.01, 0.01)	0.02 (0.01, 0.03) [a]	0.02 (0.01, 0.03) [a]	0.01 (0.00, 0.01)	0.01 (0.01, 0.02) [b]	0.01 (0.01, 0.01) [c]
MPV, fl	9.70 (9.10, 10.60)	9.60 (8.90, 10.50)	9.90 (9.10, 10.40)	10.05 (9.30, 11.20)	9.65 (9.20, 10.10)	9.60 (9.15, 10.50)
AST, U/L	22.00 (19.00, 25.00)	22.50 (17.00, 29.00)	29.00 (20.50, 46.00) [a]	25.00 (22.00, 30.00) [a]	21.00 (18.00, 25.00)	23.00 (20.00, 26.50) [c]
ALT, U/L	21.50 (16.00, 31.00)	29.50 (21.00, 39.00) [a]	31.50 (20.00, 50.00) [a]	24.50 (17.00, 55.00)	21.50 (16.00, 35.00) [b]	22.00 (18.00, 40.50)
AST/ALT	1.00 (0.78, 1.26)	0.75 (0.56, 1.00) [a]	1.06 (0.72, 1.26)	1.08 (0.55, 1.38)	0.88 (0.71, 1.17) [b]	0.95 (0.71, 1.17) [c]
ALP, U/L	68.00 (56.00, 81.00)	50.00 (43.00, 63.00) [a]	47.50 (40.00, 65.50) [a]	54.50 (48.00, 75.00)	57.00 (47.00, 68.00) [ab]	59.00 (46.50, 70.50) [a]
LDH, U/L	182.00 (158.00,195.00)	167.50 (146.00, 205.00)	235.50 (189.00,334.00)[a]	185.50 (168.00,205.00)	173.00 (157.00,186.00)	177.00(165.00,193.50)[c]
γ-GT, U/L	18.00 (14.00, 27.00)	23.50 (16.00, 44.00)	23.50 (17.00, 42.00)	24.00 (17.00, 61.00)	20.00 (16.00, 31.00) [b]	19.50 (14.00, 29.50) [c]
TBIL, μmol /L	12.00 (9.50, 17.60)	9.55 (7.90, 10.30) [a]	8.80 (7.70, 11.45) [a]	14.65 (13.10, 18.20)	11.80 (9.30, 15.20) [b]	13.10 (10.65, 16.20) [c]
DBIL, μmol/L	2.80 (2.20, 4.10)	2.50 (2.00, 3.00) [a]	3.00 (2.25, 3.55)	3.35 (2.80, 4.40)	2.95 (2.50, 3.80) [b]	3.25 (2.50, 4.40) [c]
IBIL, μmol/L	9.70 (7.50, 13.60)	7.00 (6.00, 8.00) [a]	6.10 (5.15, 8.05) [a]	11.70 (9.90, 13.80)	9.00 (6.90, 11.40) [b]	9.75 (8.00, 12.45) [c]

Total protein, g/L	76.50 (73.30, 80.00)	65.90 (63.20, 70.00) [a]	63.30 (58.90, 68.20) [a]	78.35 (77.00, 80.00)	77.10 (73.60, 79.10) [b]	76.75 (75.00, 79.40) [c]
Albumin, g/L	46.60 (44.40, 48.50)	38.60 (35.70, 41.80) [a]	33.45 (28.40, 38.15) [a]	47.70 (45.20, 48.20)	46.15 (44.50, 49.40) [b]	47.15 (46.05, 49.40) [c]
Globin, g/L	29.60 (27.40, 32.20)	27.00 (25.70, 30.80) [a]	29.75 (27.05, 32.95)	30.90 (29.60, 33.70)	29.90 (27.60, 32.60) [b]	29.55 (27.90, 31.55)
Albumin/globin	1.60 (1.40, 1.70)	1.40 (1.20, 1.50) [a]	1.10 (1.00, 1.40) [a]	1.50 (1.40, 1.60)	1.60 (1.40, 1.70) [b]	1.60 (1.50, 1.70) [c]
BUN, mmol/L	4.88 (4.02, 5.79)	4.08 (3.31, 5.01) [a]	3.76 (3.15, 4.74) [a]	4.68 (4.22, 5.30)	4.38 (3.97, 5.33)	4.89 (4.17, 5.76) [c]
Creatinine, μmol/L	71.10 (62.20, 78.60)	54.85 (48.90, 60.60) [a]	67.85 (55.75, 82.15)	73.80 (57.90, 80.70)	60.65 (55.90, 68.10) [ab]	67.00 (57.30, 78.70)
UA, μmol/L	320.70 (266.70,417.10)	261.50 (197.00,315.60)[a]	236.05 (199.75,323.00)[a]	357.25 (256.00,451.60)	296.75(237.10,367.70)[b]	369.10(309.85,439.10)[ac]
Glucose, mmol/L	5.15 (4.94, 5.35)	5.19 (4.88, 5.68)	5.63 (5.24, 6.45) [a]	5.18 (5.02, 5.61)	5.14 (4.87, 5.50)	5.34 (4.96, 5.56) [c]
Mg, mmol/L	0.89 (0.86, 0.93)	0.86 (0.81, 0.89) [a]	0.82 (0.77, 0.90) [a]	0.91 (0.89, 0.94)	0.86 (0.82, 0.88) [a]	0.87 (0.83, 0.91) [c]
P, mmol/L	0.96 (0.81, 1.05)	1.21 (1.04, 1.37) [a]	1.04 (0.92, 1.31) [a]	0.96 (0.86, 1.08)	1.04 (0.94, 1.10) [b]	0.96 (0.83, 1.07) [c]
Ca, mmol/L	2.19 (2.14, 2.26)	2.10 (2.04, 2.19) [a]	1.98 (1.90, 2.07) [a]	2.20 (2.14, 2.30)	2.20 (2.16, 2.25) [b]	2.20 (2.16, 2.25) [c]
Creatine kinase, U/L	98.00 (79.00, 133.00)	63.50 (43.50, 97.00) [a]	73.00 (47.00, 117.00) [a]	95.00 (80.00, 144.00)	91.50 (71.00, 104.00) [b]	108.50 (78.00, 125.50) [c]
CK-MB activity, U/L	13.00 (10.00, 17.00)	10.00 (8.00, 12.00) [a]	12.00 (9.00, 15.00)	13.00 (10.00, 14.00)	11.00 (8.00, 13.00) [a]	12.00 (9.00, 14.00)
α-HBDH, U/L	144.00 (129.00,155.00)	133.00 (114.00, 167.50)	185.50 (153.00,287.00)[a]	145.00 (129.00,156.00)	132.00(123.00,141.00)[a]	137.00 (127.50,154.50)[c]
CO_2, mmol/L	24.50 (23.10, 26.10)	28.05 (26.70, 29.30) [a]	24.40 (22.60, 28.80)	25.05 (22.80, 27.30)	24.20 (21.70, 25.20) [b]	24.85 (23.90, 27.40)
PT, s	12.10 (11.50, 12.50)	12.90 (12.50, 13.40) [a]	12.80 (12.20, 13.50) [a]	11.80 (11.60, 12.30)	12.20 (11.90, 12.50) [b]	12.30 (11.60, 12.80) [c]
INR	0.91 (0.85, 0.95)	0.99 (0.95, 1.04) [a]	0.99 (0.93, 1.09) [a]	0.88 (0.86, 0.93)	0.92 (0.89, 0.95) [b]	0.93 (0.86, 0.98) [c]
APTT, s	35.70 (34.10, 38.40)	35.60 (33.60, 40.30)	36.50 (33.70, 39.70)	35.55 (33.50, 39.50)	37.00 (33.80, 39.10)	37.60 (35.70, 39.20)
FIB, g/l	2.98 (2.77, 3.20)	3.55 (3.08, 3.99) [a]	3.78 (3.15, 4.84) [a]	3.04 (2.82, 3.29)	3.03 (2.77, 3.34) [b]	2.97 (2.73, 3.21) [c]
TT, s	16.00 (15.50, 16.20)	15.25 (14.70, 16.20) [a]	15.30 (14.60, 15.90) [a]	16.15 (15.50, 16.40)	16.10 (15.60, 16.80) [b]	16.10 (15.70, 16.60) [c]

Definition of abbreviation: HC=health control, M=moderate, C=severe and critical, RA=recovered asymptomatic, RM=recovered moderate, RC=recovered severe and critical, CRP=C-reactive protein, WBC=white blood cell, RBC=red blood cell, MCV=mean corpuscular volume, MCH=mean corpuscular hemoglobin, MCHC=mean corpuscular hemoglobin concentration, MPV=mean platelet volume, AST=aspartate aminotransferase, ALT=alanine aminotransferase, ALP=alkaline phosphatase, LDH=lactate dehydrogenase, γ-GT=γ-glutamyl transpeptidase, TBIL=total bilirubin, DBIL=direct bilirubin, IBIL=indirect bilirubin, BUN=blood urea nitrogen, UA=urine acid, Mg=Magnesium, P=phosphorus, Ca=calcium, α-HBDH=α-hydroxybutyrate dehydrogenase, CK-MB=creatine kinase–myocardial band, PT=prothrombin time, INR=international normalized ratio, APTT= activated partial thromboplastin time, FIB=fibrinogen, TT=thrombin time.

Data was shown as median (interquartile range, *IQR*), or n (%).

Categorical variables were compared between two groups by using χ^2 test.

Comparisons were made in terms continuous variables between two groups by using *t* test for variables with a normal distribution and Wilcoxon rank sum test for variables with the non-normal distribution.

[a] $P<0.05$, HC *versus* M or C or RA or RM or RC.

[b] $P<0.05$, M *versus* RM.

[c] $P<0.05$, C *versus* RC

Table 2. Chest CT findings based on manual evaluation and artificial intelligence (AI) analysis of chest CT in healthy controls and recovered COVID-19 patients.

Variables	HC (N=26)	Recovered COVID-19 patients		
		RA (N=18)	RM(N=33)	RC (N=39)
Manual evaluation, n (%)				
Lesions	5 (19.23)	2 (27.78)	19 (57.58) [a]	26 (66.67) [a]
GGO	4 (15.38)	5 (27.78)	17 (51.52) [a]	19 (48.72) [a]
Fibrous stripe	5 (19.23)	4 (22.22)	11 (33.33)	17 (43.59) [a]
Bronchovesicular bundle distortion	0(0.00)	1 (5.56)	2 (6.06)	11 (28.21) [a]
Thickening of the adjacent pleura	0(0.00)	0(0.00)	1 (3.03)	10 (25.64) [a]
Pleural effusion	0(0.00)	0(0.00)	0(0.00)	0(0.00)
AI evaluation, median (*IQR*)				
Lesions proportion of bilateral lungs, %	0.00 (0.00, 0.00)	0.00 (0.00, 0.01)	0.00 (0.00, 0.11) [a]	0.01 (0.00, 0.09) [a]
GGO proportion of bilateral lungs, %	0.00 (0.00, 0.00)	0.00 (0.00, 0.00)	0.00 (0.00, 0.09) [a]	0.01 (0.00, 0.06) [a]
Consolidation proportion of bilateral lungs, %	0.00 (0.00, 0.00)	0.00 (0.00, 0.00)	0.00 (0.00, 0.02) [a]	0.00 (0.00, 0.01) [a]
Lesions proportion of the right lung, %	0.00 (0.00, 0.00)	0.00 (0.00, 0.02)	0.00 (0.00, 0.13) [a]	0.00 (0.00, 0.07) [a]
GGO proportion of the right lung, %	0.00 (0.00, 0.00)	0.00 (0.00, 0.00)	0.00 (0.00, 0.12) [a]	0.00 (0.00, 0.07) [a]
Consolidation proportion of the right lung, %	0.00 (0.00, 0.00)	0.00 (0.00, 0.00)	0.00 (0.00, 0.02) [a]	0.00 (0.00, 0.01) [a]
Lesions proportion of the left lung, %	0.00 (0.00, 0.00)	0.00 (0.00, 0.00)	0.00 (0.00, 0.05) [a]	0.00 (0.00, 0.09) [a]
GGO proportion of the left lung, %	0.00 (0.00, 0.00)	0.00 (0.00, 0.00)	0.00 (0.00, 0.01) [a]	0.00 (0.00, 0.08) [a]
Consolidation proportion of the left lung, %	0.00 (0.00, 0.00)	0.00 (0.00, 0.00)	0.00 (0.00, 0.00)	0.00 (0.00, 0.01)

Definition of abbreviations: COVID-19=coronavirus disease 2019, HC=healthy control, RA=recovered asymptomatic, RM=recovered moderate, RC=recovered severe and critical, AI=artificial intelligence, GGO=ground glass opacity.

Categorical variables between two groups were compared by employing χ^2 test or Fisher's exact test.

Comparisons of continuous variables between two groups were made by using Wilcoxon rank sum test because of all variables with the non-normal distribution.

[a] $P<0.05$, HC *versus* RM or RC.

Figures

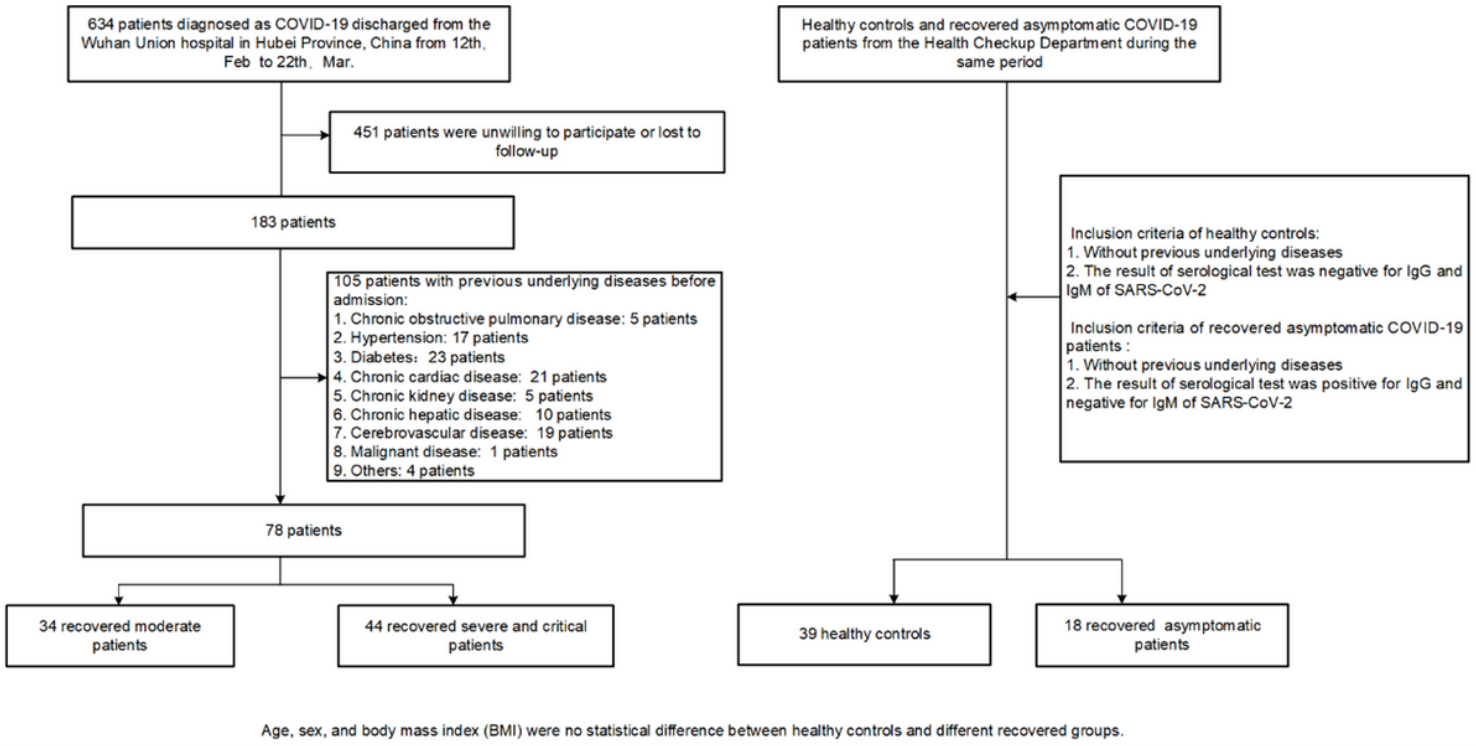

Figure 1

Inclusion Criteria. A schematic overview of the inclusion and exclusion criteria and the number of excluded subjects, and the number of patients finally included. Briefly, a total of 634 COVID-19 patients were included. 451 patients were removed from the study for either refusal to participate in loss to the follow-up. Of the remaining 183 patients, 105 patients with underlying diseases before admission were excluded. The remaining 78 patients were stratified and assigned into a RM group and a RC group based on the severity of illness at admission. Meanwhile, we included 39 HC and 18 RA patients against criteria, serving as the control group. No statistically significant differences in age, sex, and body mass index (BMI) were found between HC and different recovered groups.

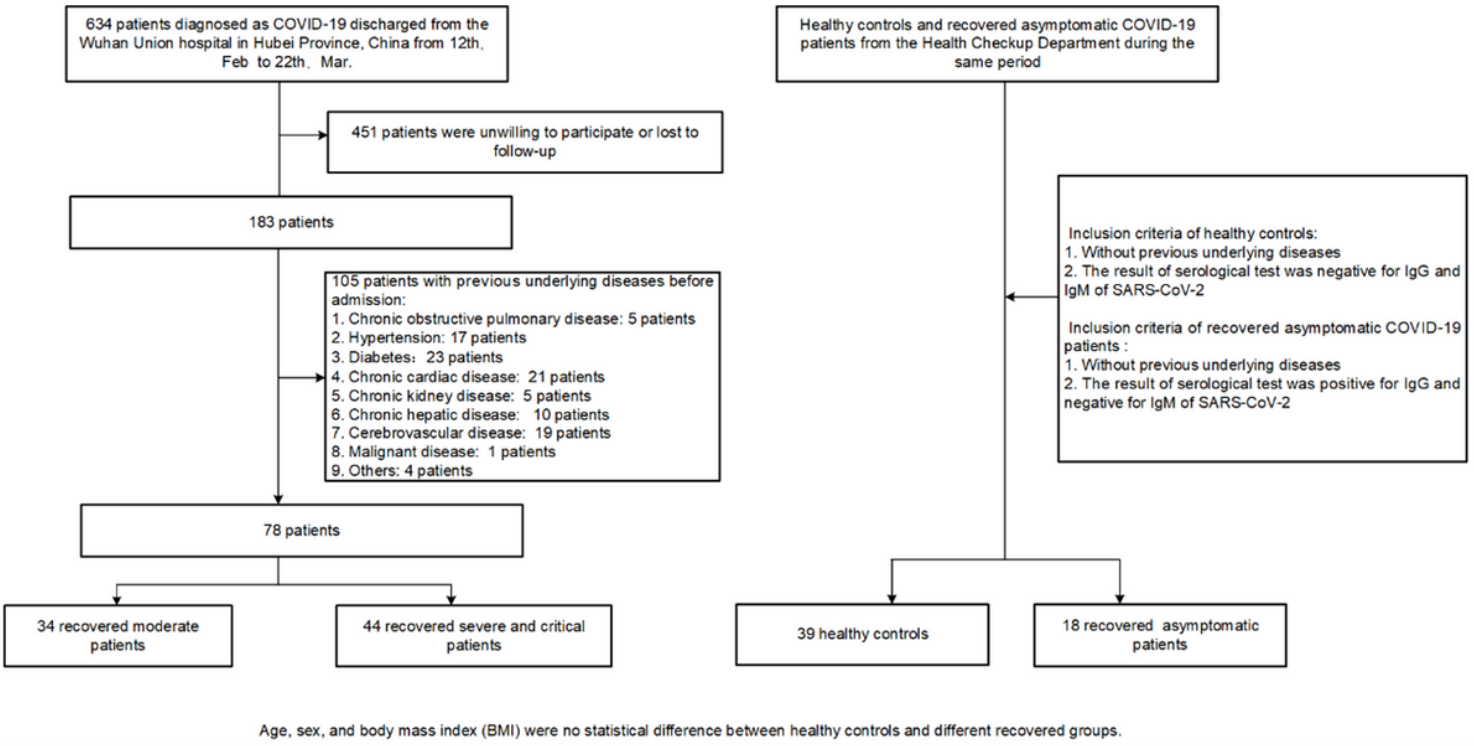

Figure 1

Inclusion Criteria. A schematic overview of the inclusion and exclusion criteria and the number of excluded subjects, and the number of patients finally included. Briefly, a total of 634 COVID-19 patients were included. 451 patients were removed from the study for either refusal to participate in loss to the follow-up. Of the remaining 183 patients, 105 patients with underlying diseases before admission were excluded. The remaining 78 patients were stratified and assigned into a RM group and a RC group based on the severity of illness at admission. Meanwhile, we included 39 HC and 18 RA patients against criteria, serving as the control group. No statistically significant differences in age, sex, and body mass index (BMI) were found between HC and different recovered groups.

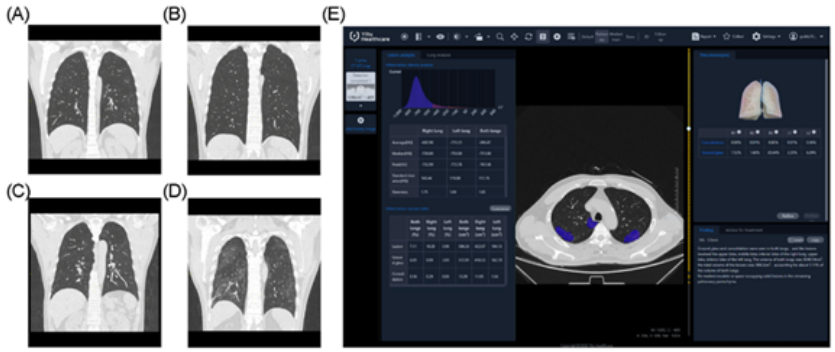

Figure 2

CT images and quantitative analysis with artificial intelligence (AI) system. Vertical scans of four patients were illustrated: (A) A 52-year-old male from HC. (B) A 54-yeal-old male from RA patients. (C) A 52-year-old male from RM patients. (D) A 53-year-old male from RC patients. (E) COVID-19 pneumonia lesions from a patient in RC group detected by the AI system are displayed with blue pseudo color.

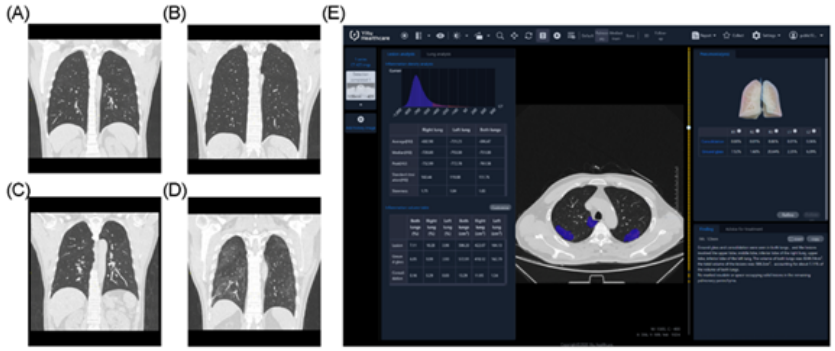

Figure 2

CT images and quantitative analysis with artificial intelligence (AI) system. Vertical scans of four patients were illustrated: (A) A 52-year-old male from HC. (B) A 54-yeal-old male from RA patients. (C) A 52-year-old male from RM patients. (D) A 53-year-old male from RC patients. (E) COVID-19 pneumonia lesions from a patient in RC group detected by the AI system are displayed with blue pseudo color.

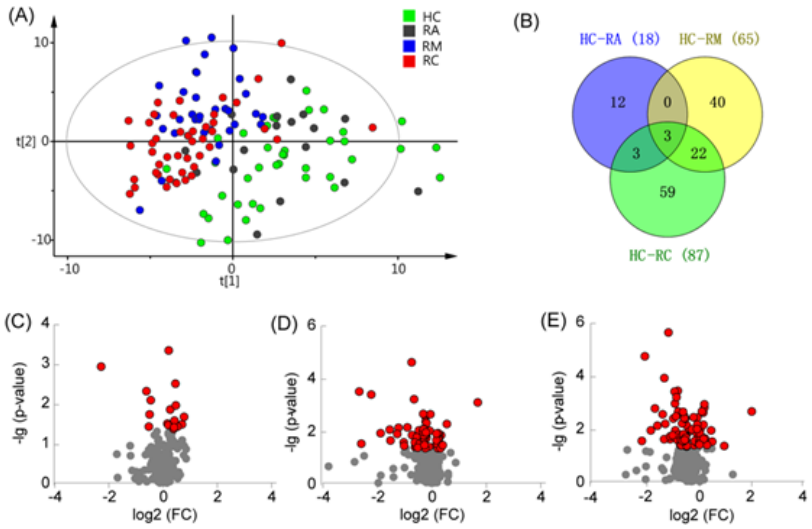

Figure 3

Profiling of metabolites from serum samples of health controls (HC), and recovered asymptomatic (RA), moderate (RM), severe and critical (RC) COVID-19 patients 3 months after discharge from hospital. (A) Score plots of PLS-DA based on the 332 metabolites detected in the four groups. (B) Venn diagram showing the number of differential metabolites in HC and RA, RM, RC patients. (C)-(E) Vocano plots of alterations of differential metabolites in RA, RM, and RC patients as compared with HC. The x-axis is the value of log2(FC), FC is the ratio of mean level of the metabolite in the RA, or RM, or RC patients to the mean value of HC and the y-axis is –lg (p-value). The red dots represent the metabolites with p-value<0.05.

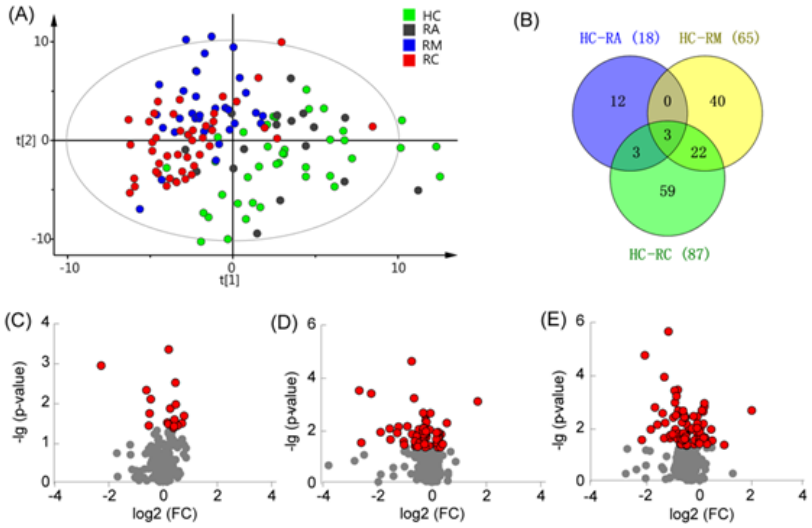

Figure 3

Profiling of metabolites from serum samples of health controls (HC), and recovered asymptomatic (RA), moderate (RM), severe and critical (RC) COVID-19 patients 3 months after discharge from hospital. (A) Score plots of PLS-DA based on the 332 metabolites detected in the four groups. (B) Venn diagram showing the number of differential metabolites in HC and RA, RM, RC patients. (C)-(E) Vocano plots of alterations of differential metabolites in RA, RM, and RC patients as compared with HC. The x-axis is the value of log2(FC), FC is the ratio of mean level of the metabolite in the RA, or RM, or RC patients to the mean value of HC and the y-axis is –lg (p-value). The red dots represent the metabolites with p-value<0.05.

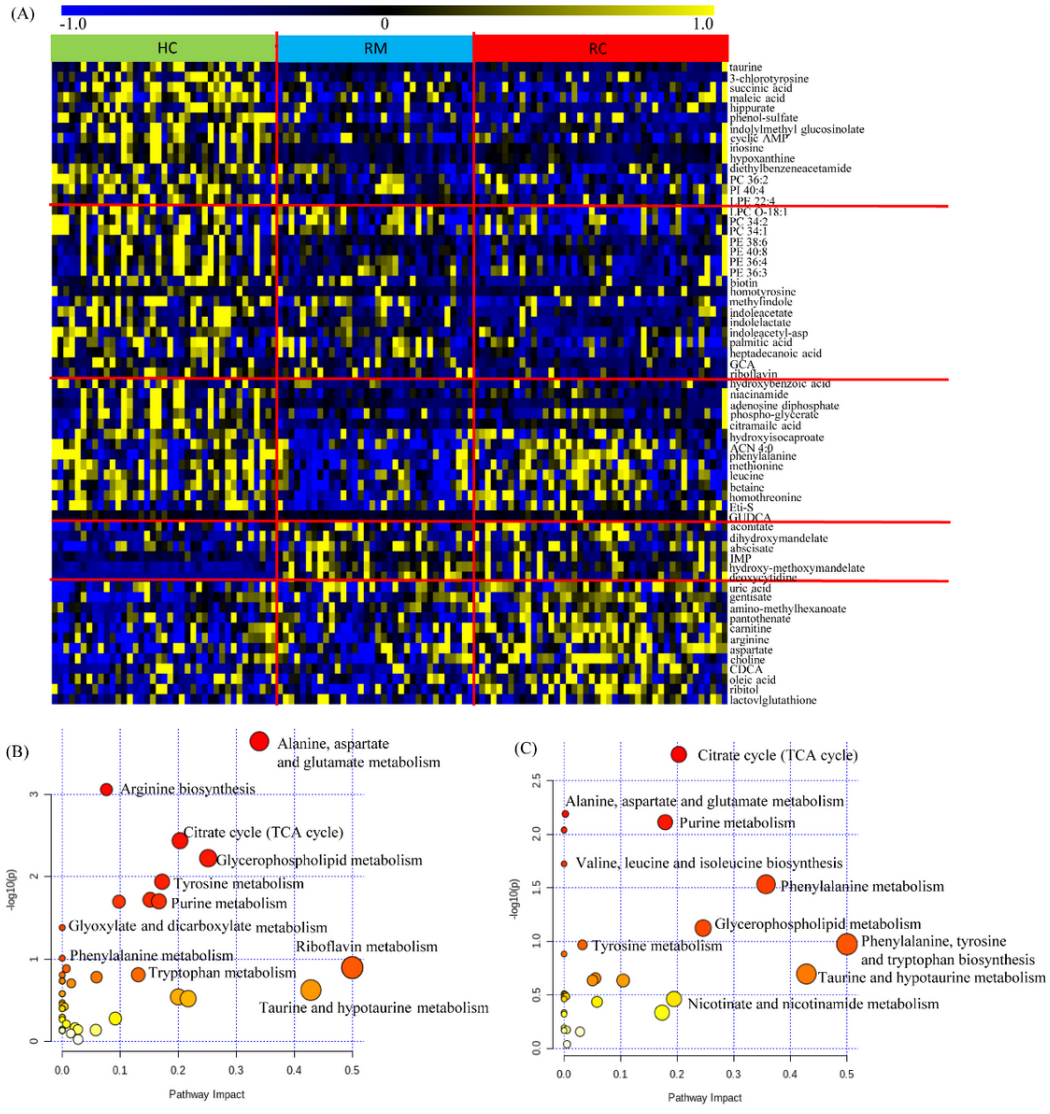

Figure 4

Significantly changed metabolites in recovered moderate (RM), severe and critical (RC) COVID-19 patients compared to health control (HC) 3 months after discharge from hospital. (A) Heat map of significantly changed metabolites in RM and RC patients as compared to HC. Only differential metabolites with P <0.01 or 0.67>FC or FC>1.5 are displayed, and the shades of the color indicate the level of metabolites (blue and yellow are indicative of relatively lower and higher level, respectively, and black shows the mean level). (C) (D) Related disturbed pathways of differential metabolites in the RM and RC patients, respectively. The value of P and pathway impact is calculated from the pathway enrichment and topology analysis, respectively. The values of P (small) and pathway impact (big) indicate that the influence of the pathway (great).

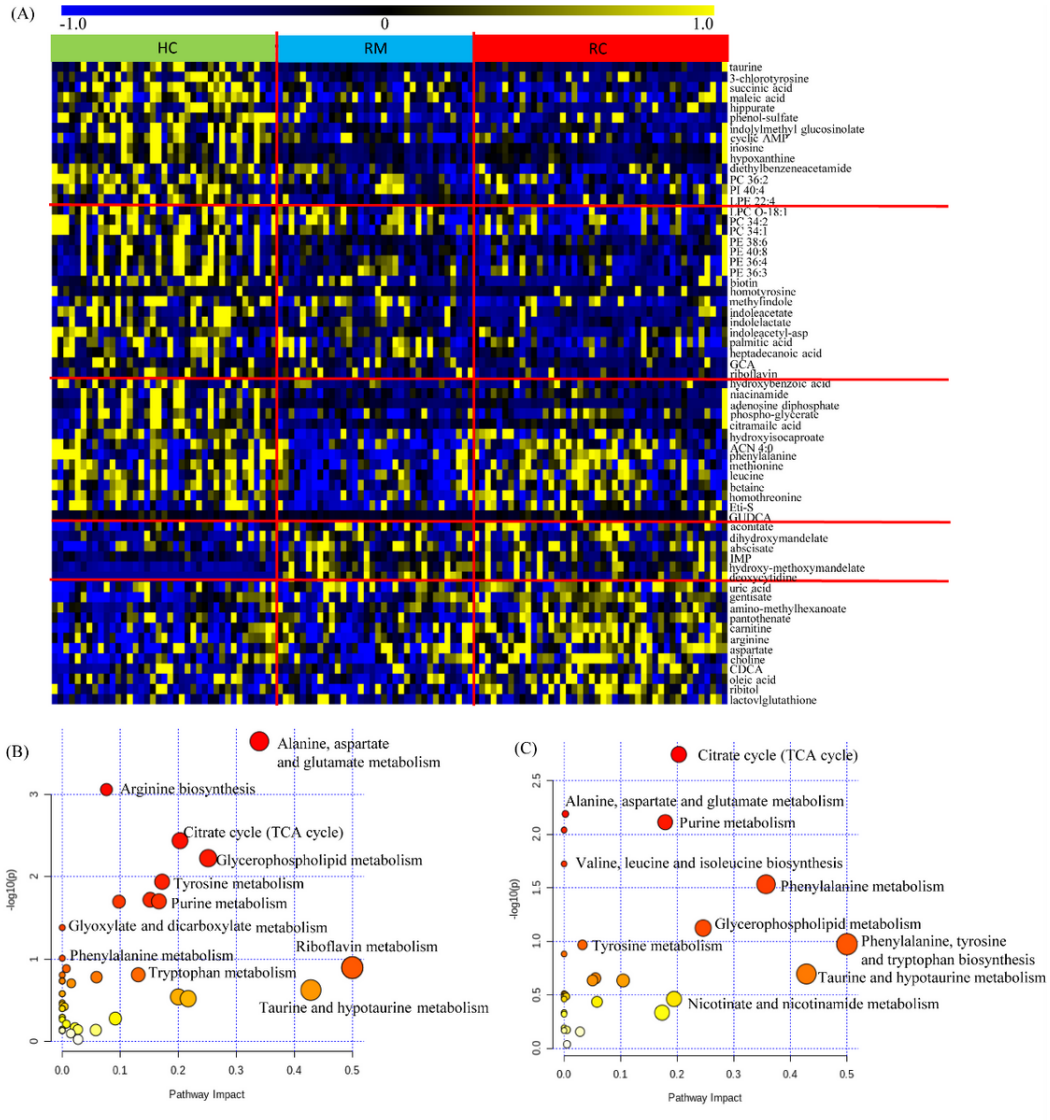

Figure 4

Significantly changed metabolites in recovered moderate (RM), severe and critical (RC) COVID-19 patients compared to health control (HC) 3 months after discharge from hospital. (A) Heat map of significantly changed metabolites in RM and RC patients as compared to HC. Only differential metabolites with P <0.01 or 0.67>FC or FC>1.5 are displayed, and the shades of the color indicate the level of metabolites (blue and yellow are indicative of relatively lower and higher level, respectively, and black shows the mean level). (C) (D) Related disturbed pathways of differential metabolites in the RM and RC patients, respectively. The value of P and pathway impact is calculated from the pathway enrichment and topology analysis, respectively. The values of P (small) and pathway impact (big) indicate that the influence of the pathway (great).

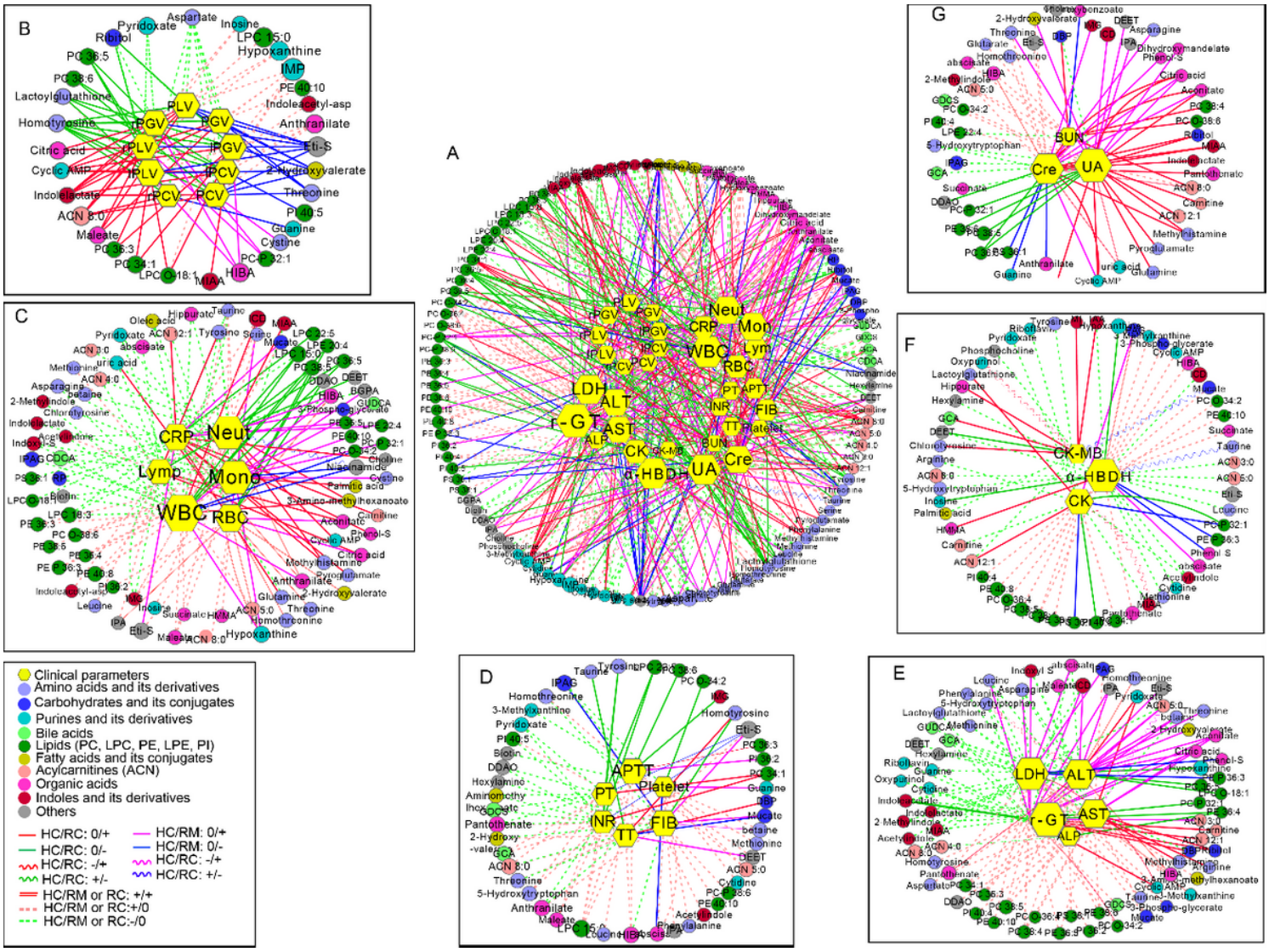

Figure 5

Network of correlations between clinical indexes and differential metabolites. Network is based on the Spearman interactions analysis between the levels of clinical indexes and differential metabolites found in recovered moderate (RM), severe and critical (RC) patients as compared to health control (HC). Only interactions with correlation coefficients > 0.3 or <-0.3, and P < 0.05 were retained. Each dot and hexagon represent a differential metabolite and a clinical index, respectively. Colors of dot indicate the species of the differential metabolites, and the size of dot and hexagon (big) is indicative of the number of interactions (higher). The colors and types of lines indicate different relationships in the HC and RM, or RC patients. For example, solid red line HC/RC: 0/+, indicates that the correlation between connected clinical index and differential metabolite (identified in the comparison between HC and RC patients) was positive (+) in the RC subjects, but without significant correlation in HC subjects. Figure A shows the total interactions between connected clinical indexes and differential metabolites in HC, RM, and RC patients. Figures B-G present the differential metabolites and clinical indexes related to the functions of lung, inflammation, coagulation state, liver, heart and kidney respectively. In the plots of C, D, E, F, the number of dash lines was greater than that of solid lines, indicating that many relationships between the differential metabolites and clinical indexes in the HC did not apply in the RM and RC patients. In the plots of B, G, the solid lines were more than that of dash lines, indicating that many differential metabolites bore unique relationships with the clinical indexes in the RM, or RC patients, which did not exist in HC.

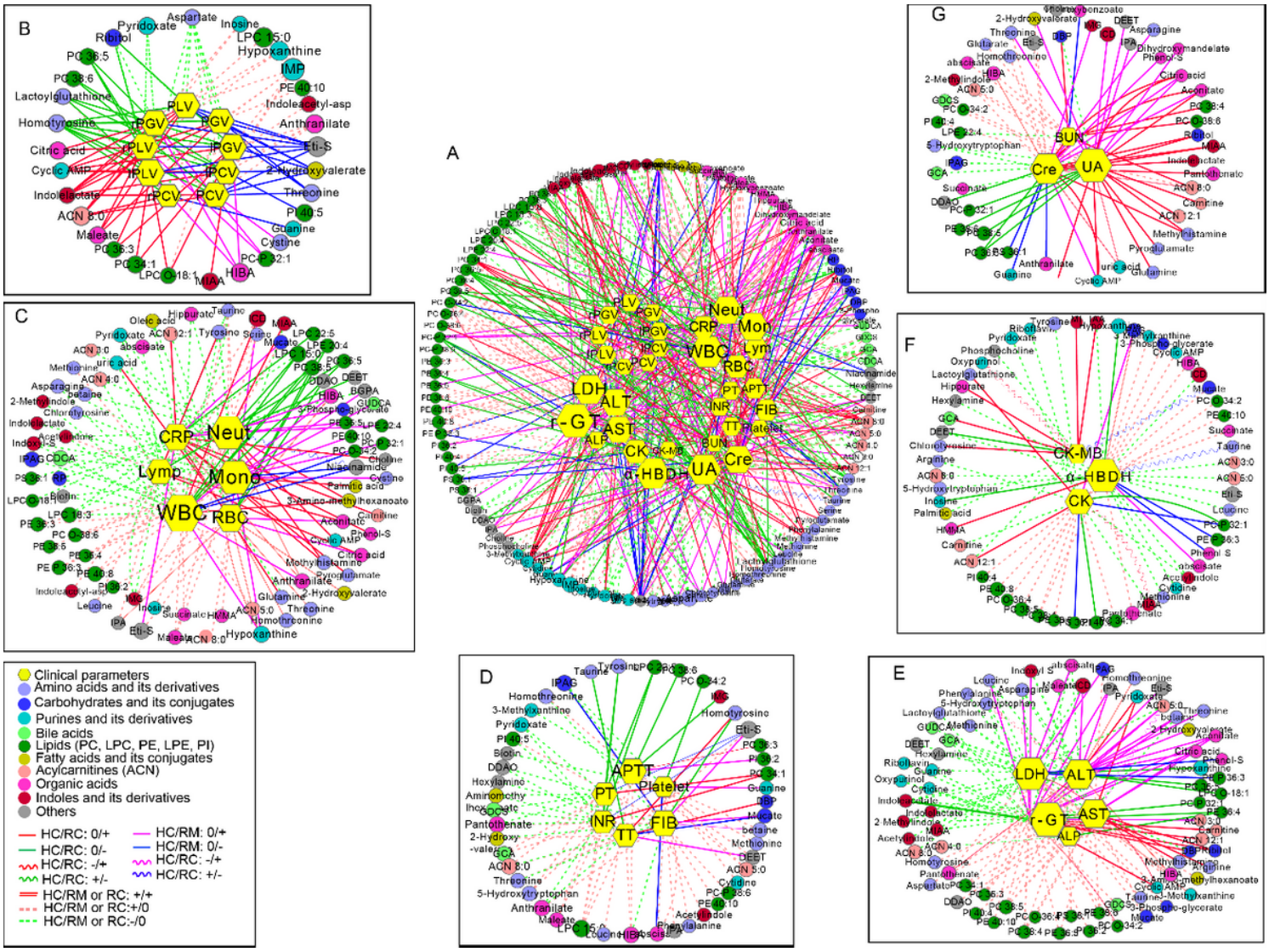

Figure 5

Network of correlations between clinical indexes and differential metabolites. Network is based on the Spearman interactions analysis between the levels of clinical indexes and differential metabolites found in recovered moderate (RM), severe and critical (RC) patients as compared to health control (HC). Only interactions with correlation coefficients > 0.3 or <-0.3, and P < 0.05 were retained. Each dot and hexagon represent a differential metabolite and a clinical index, respectively. Colors of dot indicate the species of the differential metabolites, and the size of dot and hexagon (big) is indicative of the number of interactions (higher). The colors and types of lines indicate different relationships in the HC and RM, or RC patients. For example, solid red line HC/RC: 0/+, indicates that the correlation between connected clinical index and differential metabolite (identified in the comparison between HC and RC patients) was positive (+) in the RC subjects, but without significant correlation in HC subjects. Figure A shows the total interactions between connected clinical indexes and differential metabolites in HC, RM, and RC patients. Figures B-G present the differential metabolites and clinical indexes related to the functions of lung, inflammation, coagulation state, liver, heart and kidney respectively. In the plots of C, D, E, F, the number of dash lines was greater than that of solid lines, indicating that many relationships between the differential metabolites and clinical indexes in the HC did not apply in the RM and RC patients. In the plots of B, G, the solid lines were more than that of dash lines, indicating that many differential metabolites bore unique relationships with the clinical indexes in the RM, or RC patients, which did not exist in HC.

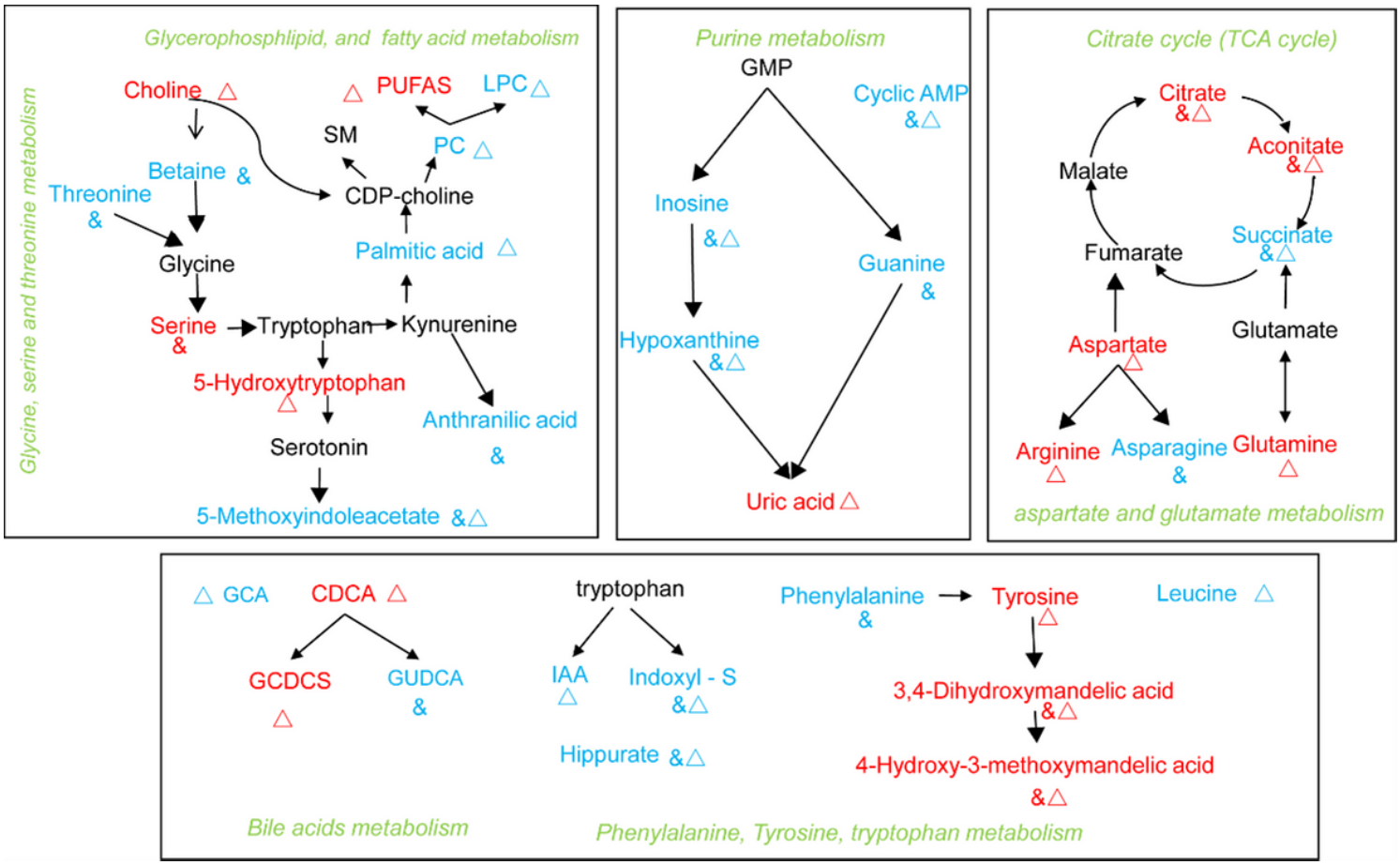

Figure 6

Main disordered pathways of differential metabolites in recovered moderate (RM), severe and critical (RC) patients when compared to health control (HC) 3 months after discharge. &, Δ the metabolite was obviously altered in the RM and RC when compared with HC, respectively. The color of blue and red for metabolites illustrated that the metabolite was increased or decreased in RM and/or RC when compared with HC, respectively.

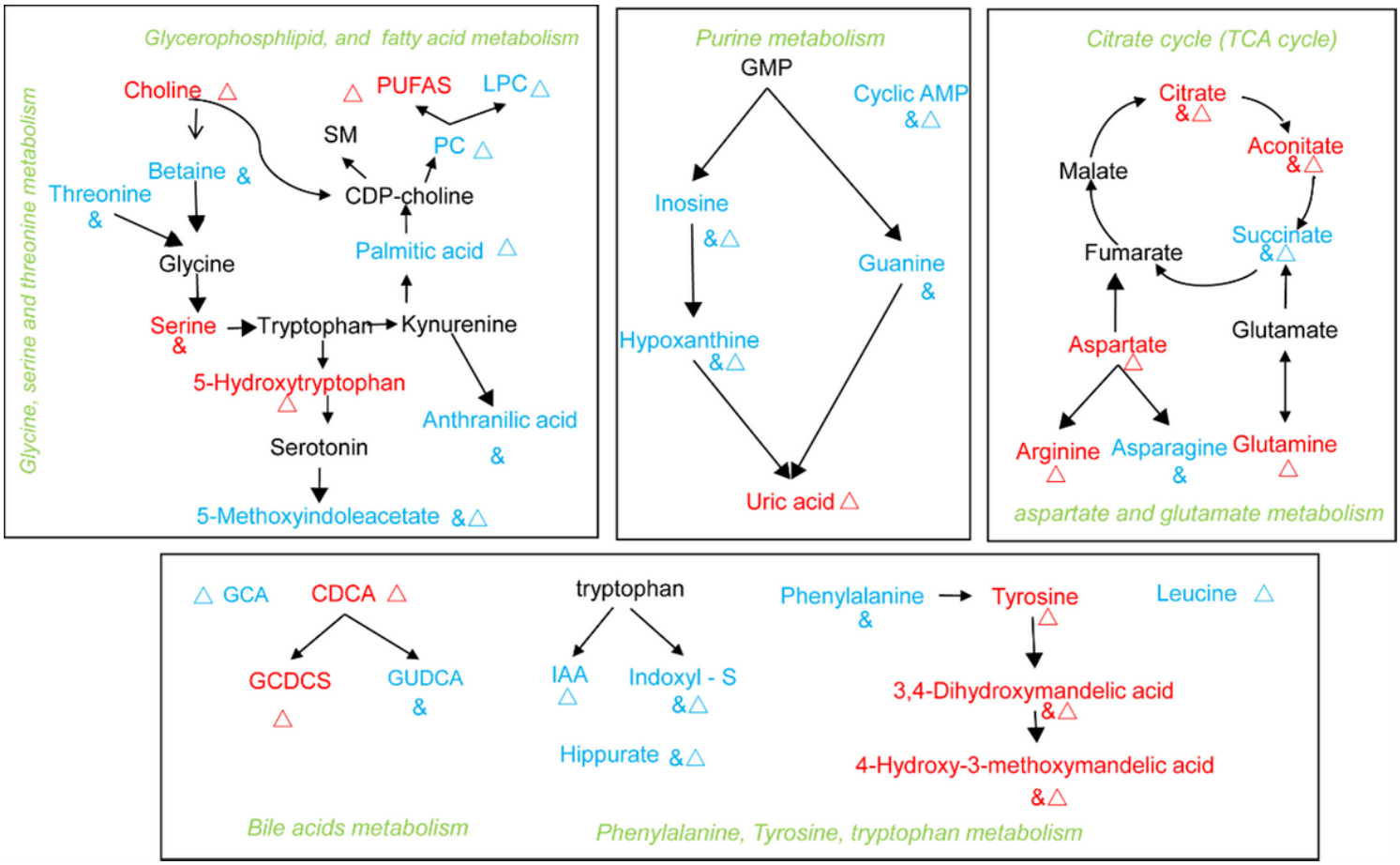

Figure 6

Main disordered pathways of differential metabolites in recovered moderate (RM), severe and critical (RC) patients when compared to health control (HC) 3 months after discharge. &, Δ the metabolite was obviously altered in the RM and RC when compared with HC, respectively. The color of blue and red for metabolites illustrated that the metabolite was increased or decreased in RM and/or RC when compared with HC, respectively.

Supplementary Files

This is a list of supplementary files associated with this preprint. Click to download.

- Supplementaryinformation.docx
- Supplementaryinformation.docx